Supporting information for:

Probing the reactivity of a transient Al(I) species

with substituted arenes

Imogen Squire, Michelangelo Tritto, Juliana Morell and Clare Bakewell

Table of contents

1. General Experimental Section

All manipulations were carried out using standard Schlenk-line and glovebox techniques under an inert atmosphere of argon. An MBraun Labmaster glovebox with an atmosphere of N_2 was employed, operating at < 0.1 ppm O_2 and < 0.1 ppm H_2O. Glassware was dried for at least 12 h at 125 °C prior to use. Toluene and hexane were dried over activated alumina from an SPS (solvent purification system) based upon the Grubbs design, stored over activated 3Å molecular sieves and sparged with argon before use. Benzene-d_6, toluene-d_8 and *ortho*-xylene were purchased dry and stored over activated 3Å molecular sieves. *Meta*-xylene and *para*-xylene were dried over CaH_2, distilled and stored over activated 3Å molecular sieves.

NMR-scale reactions were conducted in J. Young's tap tubes and prepared in a glovebox. NMR tubes were heated using DrySyn NMR tube heating block.   Capillary internal standards of ferrocene in benzene-d_6 and benzyl benzoate in toluene-d_8 were used to obtain NMR yields for **1** and **2**. [1]H (tetramethylsilane; 0 ppm) and [13]C (tetramethylsilane; 0 ppm) and ^{19}F ($CFCl_3$; 0 ppm) NMR spectra were obtained on BRUKER 400 MHz or 700 MHz (with cryoprobe) instruments; all chemical shift values are quoted in ppm. Data was processed using MestReNova software. Elemental analysis was conducted by Orfhlaith McCullough at London Metropolitan University, and has been obtained to the best of our abilities given the extremely air and moisture sensitive nature of the compounds.

Triethylamine alane and compound **A** were synthesized according to literature procedures.[1,2] The synthesis of **B** was previously reported by our research group.[3] Other chemicals were purchased from Sigma Aldrich, Fluorochem or Alfa Aeser and used without further purification.

2. Synthetic procedures

Synthetic methods to form aromatic adducts were adapted from a procedure previously reported by our group, to form an analogue of **1** with benzene-d_6.[4]

1: Compound **B** (20.7 mg, 0.04 mmol) was added to a solution of excess compound **A** (23.1 mg, 0.05 mmol) in benzene (0.6 mL) and the combined solution was transferred to a JY NMR tube. The sample was heated at 80 °C for 5 days. The solvent was removed *in vacuo*, hexane (1 mL) was added and the sample was recrystallised by slow evaporation at 25 °C. The bright red crystals were isolated and dried *in vacuo* (11.1 mg, 50 %)(NMR yield of deuterated analogue 87 %).
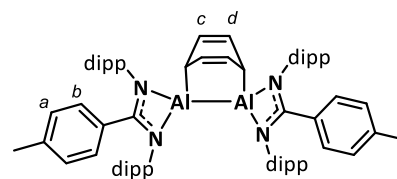
^{1}H NMR (400 MHz, C$_6$D$_6$, 298 K): δ_H 0.41 (d, 6H, CH(CH_3), $^3J_{HH}$ = 6.8 Hz), 0.51 (d, 6H, CH(CH_3), $^3J_{HH}$ = 6.8 Hz), 0.85 (d, 6H, CH(CH_3), $^3J_{HH}$ = 6.8 Hz), 1.25 (d, 6H, CH(CH_3), $^3J_{HH}$ = 6.8 Hz), 1.34 (d, 6H, CH(CH_3), $^3J_{HH}$ = 6.8 Hz), 1.41 (d, 6H, CH(CH_3), $^3J_{HH}$ = 6.8 Hz), 1.50 (d, 6H, CH(CH_3), $^3J_{HH}$ = 6.8 Hz), 1.52 (d, 6H, CH(CH_3), $^3J_{HH}$ = 6.8 Hz), 1.62 (s, 6H, *p*-CH_3), 2.76 (t, 2H, AlCH, $^3J_{HH}$ = 6.4 Hz), 3.22 (sept, 4H, CH(CH_3)$_2$, $^3J_{HH}$ = 6.8 Hz), 3.95 (sept, 2H, CH(CH_3)$_2$, $^3J_{HH}$ = 6.8 Hz), 4.07 (sept, 2H, CH(CH_3)$_2$, $^3J_{HH}$ = 6.8 Hz), 5.40 (t, 2H, CH^c=CH^d, $^3J_{HH}$ = 7.3 Hz), 6.09 (t, 2H, CH^c=CH^d, $^3J_{HH}$ = 7.3 Hz), 6.35 (d, 4H, ArH^a, $^3J_{HH}$ = 7.4 Hz), 6.85 (dd, 2H, ArH, $^3J_{HH}$ = 1.5, 7.7 Hz), 6.98 (d, 4H, ArH^b, $^3J_{HH}$ = 7.4 Hz), 7.01 (d, 2H, ArH, $^3J_{HH}$ = 7.5 Hz), 7.06 (dd, 2H, ArH, $^3J_{HH}$ = 1.5, 7.7 Hz), 7.12 (d, 2H, ArH, $^3J_{HH}$ = 7.5 Hz), 7.20-7.28 (m, 4H, ArH).

^{13}C{^{1}H} NMR (101 MHz, C$_6$D$_6$, 298 K): δ_C 20.9 (*p*-CH_3), 22.8 (CH(CH_3)$_2$), 23.3 (CH(CH_3)$_2$), 23.9 (CH(CH_3)$_2$), 24.2 (CH(CH_3)$_2$), 24.4 (CH(CH_3)$_2$), 25.5 (CH(CH_3)$_2$), 26.0 (CH(CH_3)$_2$), 26.5 (CH(CH_3)$_2$), 28.1 (CH(CH_3)$_2$), 28.4 (CH(CH_3)$_2$), 28.6 (CH(CH_3)$_2$), 28.7 (CH(CH_3)$_2$), 38.7 (AlCH), 119.8 (CH^c=CH^d), 123.5 (CH), 123.9 (CH), 124.3 (CH), 124.5 (CH), 125.8 (CH), 126.3 (CH^c=CH^d), 126.5 (CH), 126.8 (C^{IV}), 128.4 (CH), 128.6 (CH^a), 130.5 (CH^b), 139.3 (C^{IV}), 139.5 (C^{IV}), 140.7 (C^{IV}), 143.3 (C^{IV}), 143.6 (C^{IV}), 144.4 (C^{IV}), 145.3 (C^{IV}), 172.2 (NC(Ar)N).

2: Compound **B** (20.3 mg, 0.04 mmol) was added to a solution of excess compound **A** (22.2 mg, 0.05 mmol) in toluene (0.6 mL) and the combined solution was transferred to a JY NMR tube. The sample was heated at 110 °C for 4 days. The solvent was removed *in vacuo* and sample was rinsed with hexane (3 x 1 mL), yielding a red microcrystalline solid, which was dried *in vacuo* (9.3 mg, 42 %)(NMR yield of deuterated analogue 82 %).
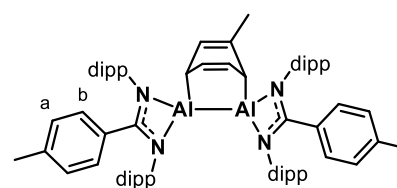
Due to the exchange effects, there are two distinct orientations for the molecule in solution, and these two orientations appear across several samples to be present in the approximate ratio major(α):minor(β) 1:0.4. Because of the complexity that this creates the NMR spectrum, ^{1}H integrations are only presented for the major orientation. Due to overlapping resonances, not all integrals are reliable and not all minor orientation resonances are visible. Minor orientation resonances marked in green.

^{1}H NMR (700 MHz, C$_6$D$_6$, 298K): δ 0.30 (d, β CH(CH_3)), 0.32, (d, 3H, CH(CH_3), $^3J_{HH}$ = 6.6 Hz), 0.36 (d, 3H, CH(CH_3), $^3J_{HH}$ = 6.6 Hz), 0.39 (d, 3H, CH(CH_3), $^3J_{HH}$ = 6.6 Hz), 0.42 (d, β CH(CH_3)), 0.50 (d, β CH(CH_3)), 0.54 (d, 3H, CH(CH_3), $^3J_{HH}$ = 6.6 Hz), 0.75 (d, 3H, CH(CH_3), $^3J_{HH}$ = 6.6 Hz), 0.91 (d, β CH(CH_3)),

0.93 (d, 3H, CH(CH_3), $^3J_{HH}$ = 6.6 Hz), 0.99 (d, β CH(CH_3)), 1.25 (d, 3H, CH(CH_3), $^3J_{HH}$ = 6.6 Hz), 1.28 (d, 3H, CH(CH_3), $^3J_{HH}$ = 6.6 Hz), 1.31 (d, 3H, CH(CH_3), $^3J_{HH}$ = 6.6 Hz), 1.32 (d, 3H, CH(CH_3), $^3J_{HH}$ = 6.6 Hz), 1.35 (d, β CH(CH_3)), 1.40 (d, β CH(CH_3)), 1.41 (d, 3H, CH(CH_3), $^3J_{HH}$ = 6.6 Hz), 1.42 (s, 3H, C=C-CH_3) 1.47 – 1.51 (m, 9H, CH(CH_3)), 1.52 – 1.54 (m, 6H, CH(CH_3)), 1.57 (d, β CH(CH_3)), 1.62 (s, 6H, p-CH_3), 1.64 (s, β p-CH_3), 1.98 (s, β C=C-CH_3), 2.57 (d, 1H, AlCH, $^3J_{HH}$ = 6.8 Hz), 2.65 (m, β AlCH), 2.78 (t, 1H, AlCH, $^3J_{HH}$ = 6.8 Hz), 3.10 – 3.35 (m, α+β CH(CH$_3$)$_2$ 5H), 3.87 – 4.20 (m, α+β CH(CH$_3$)$_2$ 5H), 5.14 (d, β CH=CH), 5.38 (t, β CH=CH), 5.50 (t, 1H, CH=CH, $^3J_{HH}$ = 6.8 Hz), 5.81 (d, 1H, CH=CH, $^3J_{HH}$ = 6.8 Hz), 6.20 (t, 1H, CH=CH, $^3J_{HH}$ = 6.8 Hz), 6.27 (t, β CH=CH), 6.35 (d, 2H, ArH_a, $^3J_{HH}$ = 7.8 Hz), 6.81 – 6.85 (m, 2H, ArH), 6.87 (d, β ArH), 6.94 (d, β ArH), 6.99 (m, 6H, ArH), 7.07 (d, 3H, ArH, $^3J_{HH}$ = 7.8 Hz), 7.13 (d, 3H, ArH, $^3J_{HH}$ = 7.8 Hz), 7.23 – 7.33 (m, 6H, ArH).

^{13}C{^{1}H} NMR (176 MHz, C$_6$D$_6$, 298 K): δ$_C$ 20.6 (p-CH$_3$), 22.2 (CH(CH$_3$), 22.5 (α C=C(CH$_3$)), 22.8 (C=C-CH$_3$), 23.2 (CH(CH$_3$), 23.5 (β C=C(CH$_3$)), 23.6 (CH(CH_3)),23.8 (CH(CH$_3$), 24.2 (CH(CH$_3$), 24.7 (CH(CH$_3$), 24.8 (CH(CH$_3$), 25.1 (CH(CH$_3$), 25.5 (CH(CH$_3$), 25.7 (CH(CH$_3$), 25.9 (CH(CH$_3$), 26.2 (CH(CH$_3$), 27.6 (CH(CH$_3$)$_2$), 27.7 (CH(CH$_3$)$_2$), 27.9 (CH(CH$_3$)$_2$), 28.0 (CH(CH$_3$)$_2$), 28.1 (CH(CH$_3$)$_2$), 28.2 (CH(CH$_3$)$_2$), 28.3 (CH(CH$_3$)$_2$), 28.4 (CH(CH$_3$)$_2$), 28.5 (CH(CH$_3$)$_2$), 37.4 (β AlCH), 37.6 (α AlCH), 42.6 (α AlCH), 43.3 (β AlCH), 114.4 (β CH=CH), 119.8 (β CH=CH), 120.7 (α CH=CH), 121.2 (α CH=CH), 123.2 (CH) , 123.5 (CH), 123.7 (CH), 124.0 (CH), 124.3 (CH), 124.4 (CH), 125.2 (CH), 125.3(CH), 126.0 (CH), 126.4 (α CH=CH), 126.6 (CH), 126.7 (CH), 128.3 (β CH=CH), 130.0 (CH), 130.3 (CH), 130.4 (CH), 133.4 (C=C(CH$_3$)), 139.2 (C^{IV}), 139.3 (C^{IV}), 139.7 (C^{IV}), 140.1 (C^{IV}), 140.6 (C^{IV}), 140.8 (C^{IV}), 142.8 (C^{IV}), 143.1 (C^{IV}), 143.2 (C^{IV}), 143.4 (C^{IV}), 143.8 (C^{IV}), 143.8 (C^{IV}), 144.5 (C^{IV}), 144.9 (C^{IV}), 145.4 (C^{IV}), 145.5 (C^{IV}), 145.6(C^{IV}), 171.5 (NC(Ar)N), 171.6 (NC(Ar)N), 171.9 (NC(Ar)N).

Elemental analysis expected for C$_{71}$H$_{90}$Al$_2$N$_4$: C, 80.95; H, 8.61; N, 5.32. Found: C, 78.70; H 8.53; N, 4.76.

3: Compound **B** (26.6 mg, 0.06 mmol) was added to a solution of excess compound **A** (29.2 mg, 0.07 mmol) in o-xylene (0.6 mL) and the combined solution was transferred to a JY NMR tube. The sample was heated at 80 °C for 8 days. The solvent was removed *in vacuo* and sample was recrystallised by slow evaporation from hexane. Due to co-crystallisation of a side product, these crystals were then rinsed with hexane, and dried *in vacuo* to give a red microcrystalline solid (6.8 mg, 23 %).
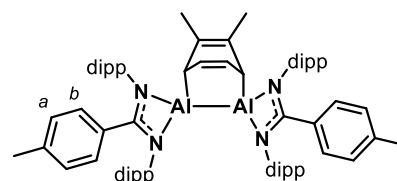
^{1}H NMR (400 MHz, C$_6$D$_6$, 298 K): δ$_H$ 0.27 (d, 3H, CH(CH_3), $^3J_{HH}$ = 6.8 Hz), 0.32 (d, 3H, CH(CH_3), $^3J_{HH}$ = 6.8 Hz), 0.38 (d, 3H, CH(CH_3), $^3J_{HH}$ = 6.8 Hz), 0.55 (d, 3H, CH(CH_3), $^3J_{HH}$ = 6.8 Hz), 0.81 (d, 3H, CH(CH_3), $^3J_{HH}$ = 6.8 Hz), 1.05 (d, 3H, CH(CH_3), $^3J_{HH}$ = 6.8 Hz), 1.15 (d, 3H, CH(CH_3), $^3J_{HH}$ = 6.8 Hz), 1.30 (d, 3H, CH(CH_3), $^3J_{HH}$ = 6.8 Hz), 1.32 (d, 3H, CH(CH_3), $^3J_{HH}$ = 6.8 Hz), 1.35 (d, 3H, CH(CH_3), $^3J_{HH}$ = 6.8 Hz), 1.41 (d, 3H, CH(CH_3), $^3J_{HH}$ = 6.8 Hz), 1.42 (s, 3H, CH=CH-CH_3), 1.46 (d, 3H, CH(CH_3), $^3J_{HH}$ = 6.8 Hz), 1.49 (d, 6H, CH(CH_3), $^3J_{HH}$ = 6.8 Hz), 1.52 (d, 3H, CH(CH_3), $^3J_{HH}$ = 6.8 Hz), 1.64 (s, 3H, p-CH_3), 1.65 (s, 3H, p-CH_3), 2.02 (s, 3H, CH=CH-CH_3), 2.58 (d, 1H, AlCH, $^3J_{HH}$ = 6.4), 2.75 (d, 1H, AlCH, $^3J_{HH}$ = 6.4), 3.06 – 3.23 (m, 3H, CH(CH$_3$)$_2$), 3.29 – 3.42 (m, 1H, CH(CH$_3$)$_2$), 3.88 – 3.97 (m, 1H, CH(CH$_3$)$_2$), 3.97 – 4.09 (m, 2H, CH(CH$_3$)$_2$), 4.13 – 4.25 (m, 1H, CH(CH$_3$)$_2$), 5.44 (t, 1H, CH=CH, $^3J_{HH}$ = 7.4), 6.25 – 6.42 (m, 5H, ArH^e and

CH=C*H*), 6.84 – 6.90 (m, 2H, Ar*H*), 6.97 – 7.05 (m, 4H, Ar*H*), 7.05 – 7.09 (m, 2H, Ar*H*), 7.11 – 7.15 (m, 2H, Ar*H*), 7.23 – 7.38 (m, 4H, Ar*H*).

Note: One of the presumed CH=CH resonances (δ_H = 6.31) is coincident with the aromatic CHs on the p-tol backbone – chemical shift determined from COSY but splitting (presumed triplet) is unobservable. Aromatic region is poorly resolved and two protons are unaccounted for, likely due to being obscured by the residual C_6D_5H.

^{13}C NMR (101 MHz, C_6D_6) δ 19.2 (*p*-*C*H$_3$), 20.9(C=C(*C*H$_3$)), 22.5 (CH(*C*H$_3$)), 23.6(CH(*C*H$_3$)), 24.1 (CH(*C*H$_3$)), 24.7 (C=C(*C*H$_3$)), 24.8 (CH(*C*H$_3$)), 25.3 (CH(*C*H$_3$)), 25.5 (CH(*C*H$_3$)), 26.0 (CH(*C*H$_3$)), 26.3 (CH(*C*H$_3$)), 27.9 (*C*H(CH$_3$)$_2$), 28.3 (*C*H(CH$_3$)$_2$), 28.4 (*C*H(CH$_3$)$_2$), 28.6 (*C*H(CH$_3$)$_2$), 29.0 (*C*H(CH$_3$)$_2$), 44.4 (Al*C*H), 45.3 (Al*C*H), 120.1 (CH=*C*H), 121.4 (CH=*C*H), 123.8 (*C*H), 124.1 (*C*H), 124.4 (*C*H), 124.6 (*C*H), 125.0 (*C*H), 125.3 (*C*H), 125.7 (*C*H), 126.3 (*C*H), 126.4 (*C*H), 126.7 (*C*H), 130.7(*C*H^a), 130.9 (*C*H^b), 139.3 (*C*^{IV}), 139.9 (*C*^{IV}), 140.8 (*C*^{IV}), 143.1 (*C*^{IV}), 143.5 (*C*^{IV}), 144.5 (*C*^{IV}), 144.8 (*C*^{IV}), 145.7 (*C*^{IV}), 171.4 (N*C*(Ar)N), 172.2 (N*C*(Ar)N).

Elemental analysis expected for $C_{72}H_{92}Al_2N_4$: C, 81.01; H, 8.69; N, 5.25. Found: C, 79.39; H 8.61; N, 4.22.

4: Compound **B** (16.8 mg, 0.03 mmol) was added to a solution of excess compound **A** (19.5 mg, 0.04 mmol) in *m*-xylene (0.6 mL) and the combined solution was transferred to a JY NMR tube. The sample was heated at 100 °C for 5 days. The solvent was removed *in vacuo*, hexane was added and sample was filtered, before being recrystallised by slow evaporation at 25 °C. Product co-crystallised with ^{dipp}BDIAlH$_2$ and was separated by washing with hexane, yielding dark red crystals (3.2 mg, 17%).
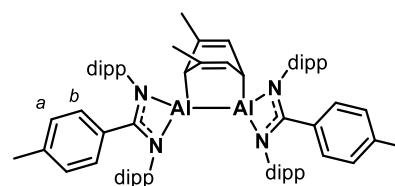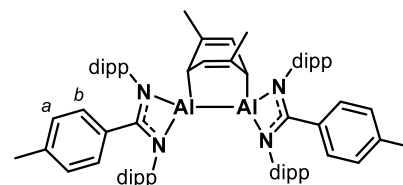

^{1}H NMR (700 MHz, C_6D_6) δ 0.30 (d, 3H, CH(C*H$_3$*), $^3J_{HH}$ = 6.8 Hz), 0.34 (d, 3H, CH(C*H$_3$*), $^3J_{HH}$ = 6.8 Hz), 0.41 (d, 3H, CH(C*H$_3$*), $^3J_{HH}$ = 6.8 Hz), 0.52 (d, 3H, CH(C*H$_3$*), $^3J_{HH}$ = 6.8 Hz), 0.89 (d, 3H, CH(C*H$_3$*), $^3J_{HH}$ = 6.8 Hz), 1.04 (d, 3H, CH(C*H$_3$*), $^3J_{HH}$ = 6.8 Hz), 1.24 (d, 3H, CH(C*H$_3$*), $^3J_{HH}$ = 6.8 Hz), 1.26 (d, 3H, CH(C*H$_3$*), $^3J_{HH}$ = 6.8 Hz), 1.28 (d, 3H, CH(C*H$_3$*), $^3J_{HH}$ = 6.8 Hz), 1.33 (d, 3H, CH(C*H$_3$*), $^3J_{HH}$ = 6.8 Hz), 1.40 (s, 3H, C=C-C*H$_3$*), 1.47 (d, 3H, CH(C*H$_3$*), $^3J_{HH}$ = 6.8 Hz), 1.49 (d, 3H, CH(C*H$_3$*), $^3J_{HH}$ = 6.8 Hz), 1.52 (d, 3H, CH(C*H$_3$*), $^3J_{HH}$ = 6.8 Hz), 1.53 (d, 3H, CH(C*H$_3$*), $^3J_{HH}$ = 6.8 Hz), 1.54 (d, 3H, CH(C*H$_3$*), $^3J_{HH}$ = 6.8 Hz), 1.58 (d, 3H, CH(C*H$_3$*), $^3J_{HH}$ = 6.8 Hz), 1.62 (s, 3H, *p*-C*H$_3$*) , 1.63 (s, 3H, *p*-C*H$_3$*), 2.04 (s, 3H, C=C-C*H$_3$*), 2.44 (s, 1H, AlC*H*(C(CH$_3$))$_2$) , 2.71 (t, 1H, AlC*H*(CH)$_2$, $^3J_{HH}$ = 6.5 Hz), 3.13 (p, 1H, C*H*(CH$_3$)$_2$, $^3J_{HH}$ = 6.8 Hz), 3.20 (sept, 1H, C*H*(CH$_3$)$_2$, $^3J_{HH}$ = 6.8 Hz), 3.27-3.29 (m, 2H, C*H*(CH$_3$)$_2$), 3.94-3.40 (m, 2H, C*H*(CH$_3$)$_2$), 4.13 (sept, 1H, C*H*(CH$_3$)$_2$, $^3J_{HH}$ = 6.8 Hz), 4.21 (sept, 1H, C*H*(CH$_3$)$_2$, $^3J_{HH}$ = 6.8 Hz), 5.27 (d, 1H, C*H*=C(CH$_3$), $^3J_{HH}$ = 6.5 Hz), 6.03 (d, 1H, C*H*=C(CH$_3$), $^3J_{HH}$ = 6.5 Hz), 6.34 (d, 4H, Ar*H^a*, $^3J_{HH}$ = 6.5 Hz) , 6.82 – 6.88 (m, 2H, Ar*H*), 6.96 (d, 4H, Ar*H^b*, $^3J_{HH}$ = 6.5 Hz), 6.97 – 7.04 (m, 3H, Ar*H*), 7.05 – 7.11 (m, 3H, Ar*H*), 7.24 – 7.37 (m, 5H, Ar*H*).

^{13}C NMR (176 MHz, C_6D_6) δ 20.9 (*p*-*C*H$_3$), 22.7 (C=C(*C*H$_3$)), 22.8 (CH(*C*H$_3$)), 23.1 (CH(*C*H$_3$)), 23.5 (CH(*C*H$_3$)), 24.1 (C=C(*C*H$_3$)), 24.3 (CH(*C*H$_3$)), 24.6 (CH(*C*H$_3$)), 24.8 (CH(*C*H$_3$)), 24.9 (CH(*C*H$_3$)), 25.9 (CH(*C*H$_3$)), 26.1 (CH(*C*H$_3$)), 26.5 (CH(*C*H$_3$)), 28.1 (*C*H(CH$_3$)$_2$), 28.2 (*C*H(CH$_3$)$_2$), 28.3 (*C*H(CH$_3$)$_2$), 28.6 (*C*H(CH$_3$)$_2$), 28.8 (*C*H(CH$_3$)$_2$), 29.2 (*C*H(CH$_3$)$_2$), 37.5 (Al*C*H(CH)$_2$), 48.3 (Al*C*H(C(CH$_3$))$_2$), 116.7

(C*H*=C(CH$_3$)), 123.5 (C*H*=C(CH$_3$)), 123.8 (*C*H), 124.1 (*C*H), 124.4 (*C*H), 124.6 (*C*H), 124.7 (*C*H), 125.2 (*C*H), 125.6 (*C*H), 126.3 (*C*H), 126.9 (*C*H), 127.1 (*C*H), 128.4 (*C*H), 129.3 (*C*H), 130.5 (*C*H), 134.3 (*C*^{IV}), 139.3 (*C*^{IV}), 139.8 (*C*^{IV}), 140.1 (*C*^{IV}), 140.5 (*C*^{IV}), 140.6 (*C*^{IV}), 140.8 (*C*^{IV}), 143.0 (*C*^{IV}), 143.2 (*C*^{IV}), 143.5 (*C*^{IV}), 144.0 (*C*^{IV}), 144.2 (*C*^{IV}), 145.1 (*C*^{IV}), 145.7 (*C*^{IV}), 171.8 (N*C*(Ar)N), 172.2 (N*C*(Ar)N).

5: Compound **B** (17.7 mg, 0.05 mmol) was added to a solution of excess compound **A** (17.8 mg, 0.04 mmol) in *p*-xylene (0.6 mL) and the combined solution was transferred to a JY NMR tube. The sample was heated at 100 °C for 5 days. The solvent was removed *in vacuo*, hexane was added and sample was filtered, before being recrystallised by slow evaporation at 25 °C. Product co-crystallised with ^{dipp}BDIAlH$_2$ and was separated by washing with hexane, yielding dark red crystals (3.1 mg, 16%).

^{1}H NMR (400 MHz, C$_6$D$_6$) δ 0.31 (d, 6H, CH(C*H*$_3$), $^3J_{HH}$ = 6.8 Hz), 0.41 (d, 6H, CH(C*H*$_3$), $^3J_{HH}$ = 6.8 Hz), 0.82 (d, 6H, CH(C*H*$_3$), $^3J_{HH}$ = 6.8 Hz), 1.28 (d, 6H, CH(C*H*$_3$), $^3J_{HH}$ = 6.8 Hz), 1.32 (d, 6H, CH(C*H*$_3$), $^3J_{HH}$ = 6.8 Hz), 1.43 (s, 6H, C=C-C*H*$_3$), 1.49 – 1.56 (m, 18H, CH(C*H*$_3$)), 1.63 (s, 6H, *p*-C*H*$_3$), 2.59 (d, 2H, AlC*H*, $^3J_{HH}$ = 7.0 Hz), 3.13 (sept, 2H, C*H*(CH$_3$)$_2$, $^3J_{HH}$ = 6.8 Hz), 3.22 (sept, 2H, C*H*(CH$_3$)$_2$, $^3J_{HH}$ = 6.8 Hz), 3.89 (sept, 2H, C*H*(CH$_3$)$_2$, $^3J_{HH}$ = 6.8 Hz), 4.08 (sept, 2H, C*H*(CH$_3$)$_2$, $^3J_{HH}$ = 6.8 Hz), 5.91 (d, 2H, C*H*=C(CH$_3$), $^3J_{HH}$ = 7.0 Hz), 6.34 (d, 4H, Ar*H*^{a}, $^3J_{HH}$ = 7.7 Hz), 6.83 (d, 2H, Ar*H*, $^3J_{HH}$ = 7.7 Hz), 6.98 (d, 4H, Ar*H*^{b}, $^3J_{HH}$ = 7.7 Hz), 7.06 (d, 3H, Ar*H*, $^3J_{HH}$ = 7.7 Hz), 7.13 (d, 3H, Ar*H*, $^3J_{HH}$ = 7.7 Hz), 7.26 (t, 2H, Ar*H*, $^3J_{HH}$ = 7.7 Hz), 7.32 (d, 2H, Ar*H*, $^3J_{HH}$ = 7.7 Hz).

^{13}C NMR (101 MHz, C$_6$D$_6$) δ 20.9 (*p*-*C*H$_3$), 22.5 (C=C(*C*H$_3$)), 22.6 (CH(*C*H$_3$)), 23.9 (CH(*C*H$_3$)), 24.2 (CH(*C*H$_3$)), 24.3(CH(*C*H$_3$)), 24.8 (CH(*C*H$_3$)), 25.5 (CH(*C*H$_3$)), 26.0 (CH(*C*H$_3$)), 26.1 (CH(*C*H$_3$)), 28.1 (*C*H(CH$_3$)$_2$), 28.3 (*C*H(CH$_3$)$_2$), 28.4 (*C*H(CH$_3$)$_2$), 28.7 (*C*H(CH$_3$)$_2$), 42.1 (Al*C*H), 121.4 (*C*H=C(CH$_3$), 123.8 (*C*H), 124.1 (*C*H), 124.7 (*C*H), 124.9 (*C*H), 125.5 (*C*H), 126.3 (*C*H), 127.0 (*C*H), 128.6 (*C*H^a), 129.3, 130.5 (*C*H^b), 139.3 (*C*^{IV}), 140.4 (*C*^{IV}), 140.8 (*C*^{IV}), 142.9 (*C*^{IV}), 143.1 (*C*^{IV}), 144.0 (*C*^{IV}), 145.4 (*C*^{IV}), 172.1 (N*C*(Ar)N).

Anisole

Compound **B** (16.1 mg, 0.02 mmol) was added to a solution of excess compound **A** (15.2 mg, 0.02 mmol) in benzene, which was then removed *in vacuo.* The solid was dissolved in anisole and transferred to a JY NMR tube. The sample was heated at 80 °C for 2 days. The solvent was removed *in vacuo* and the sample was dissolved in C$_6$D$_6$, showing presence of three known literature compounds (Figure S14-S15).[5–7]
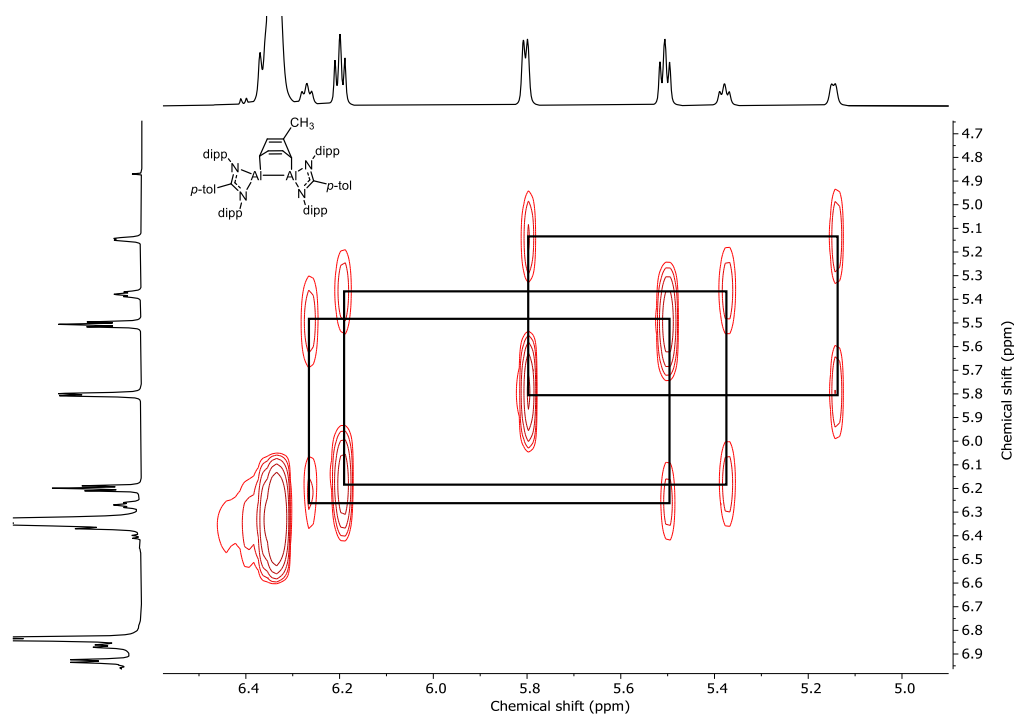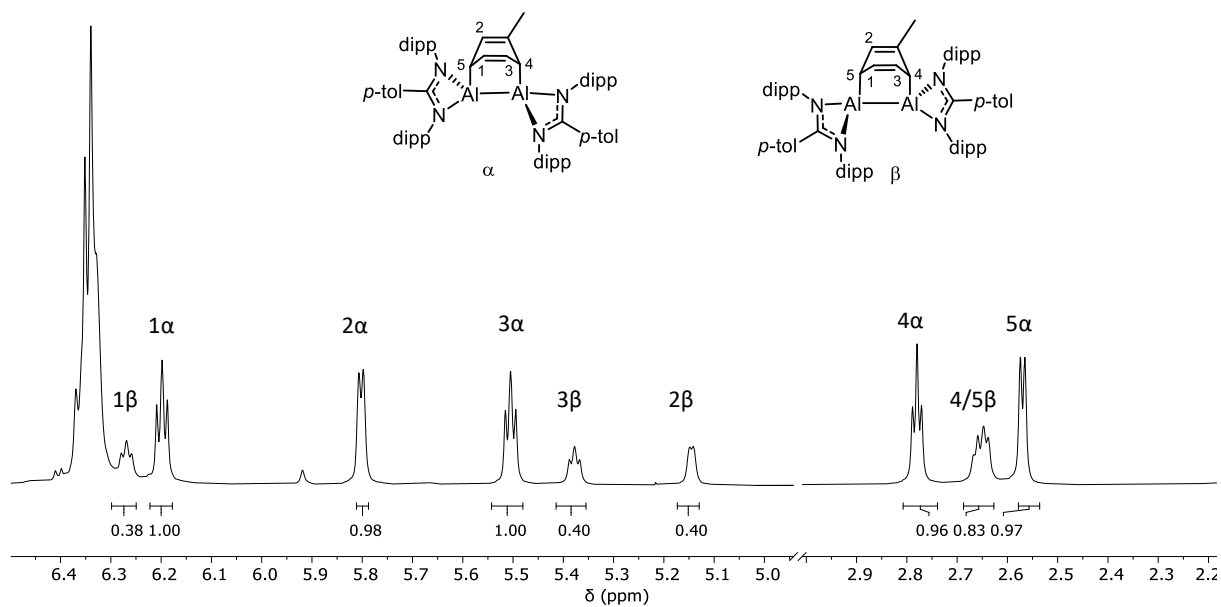
3. Supporting figures/schemes
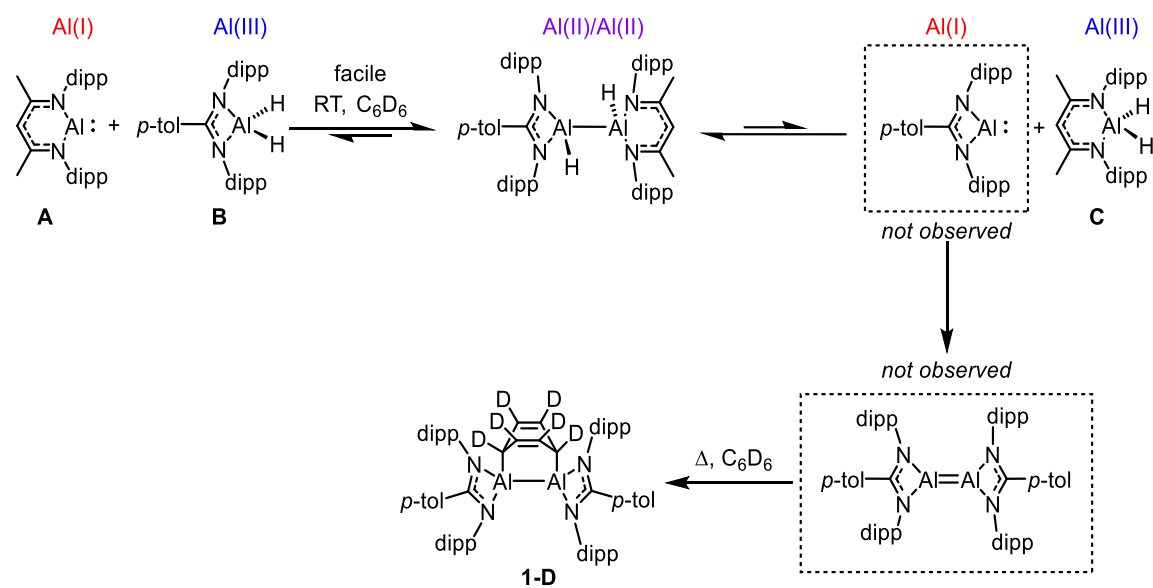
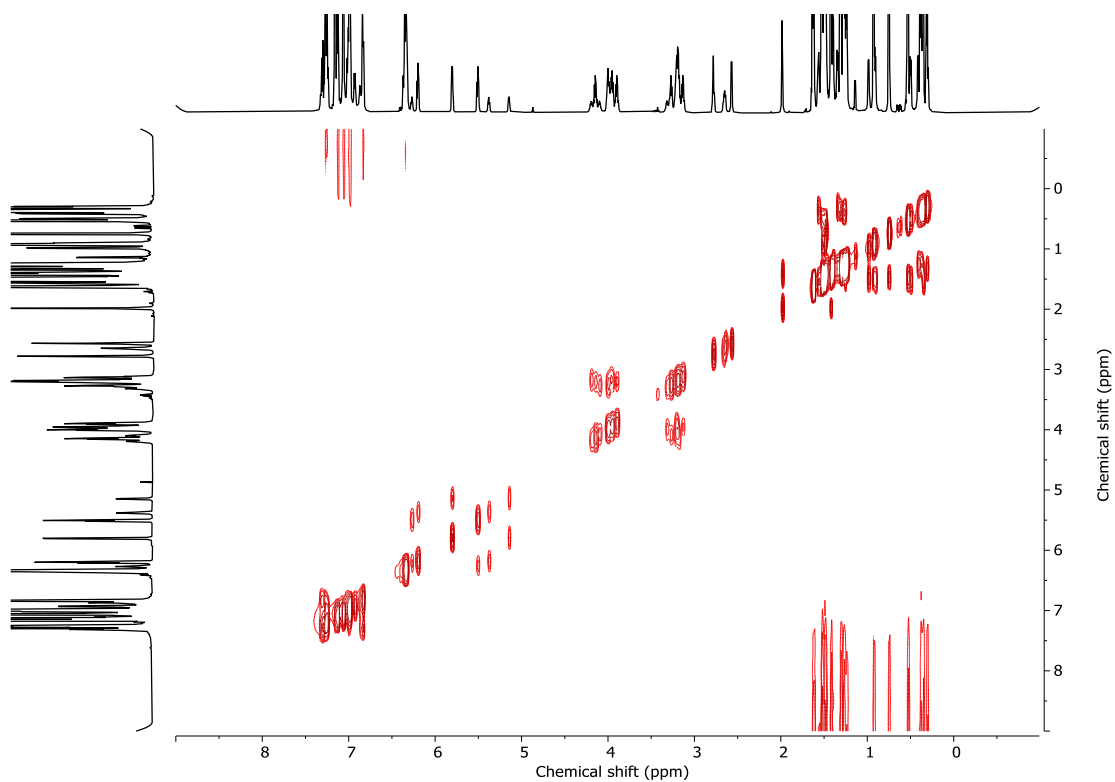

Figure S1: Proposed reaction scheme of reaction between **A** and **B** in C_6D_6, forming **1-D**
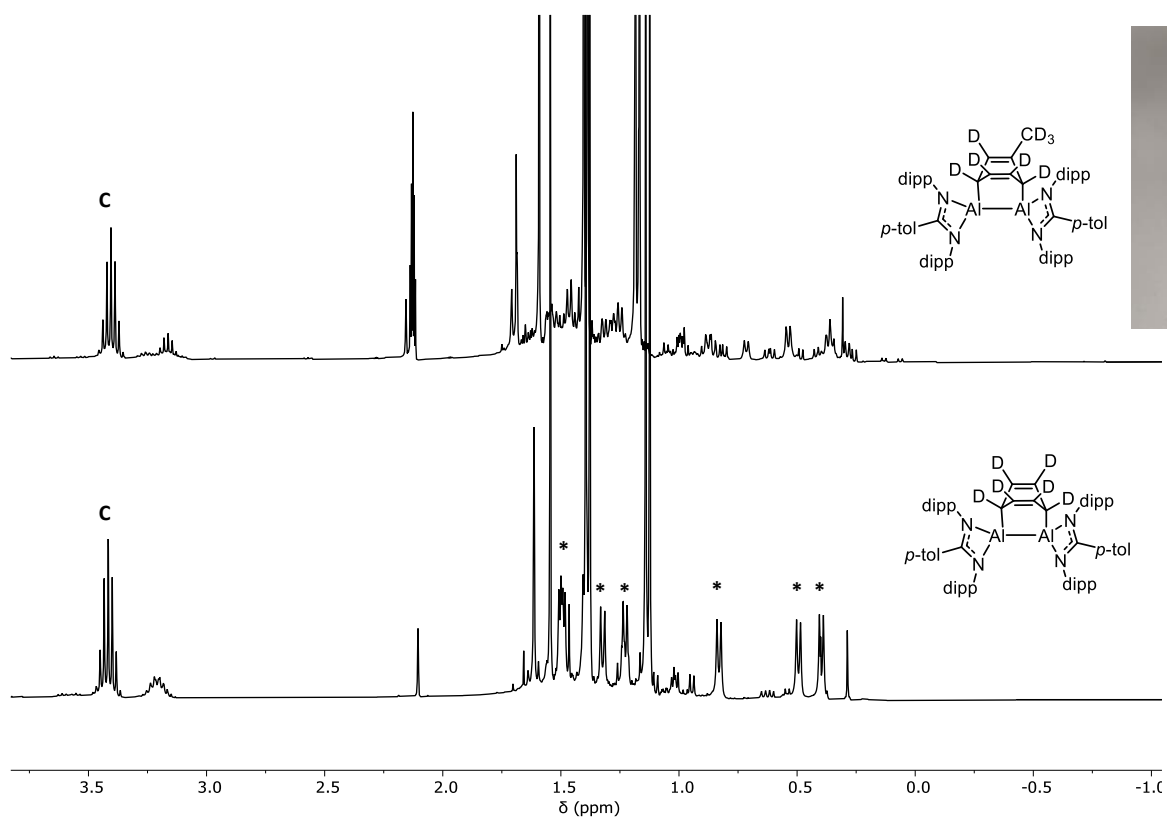
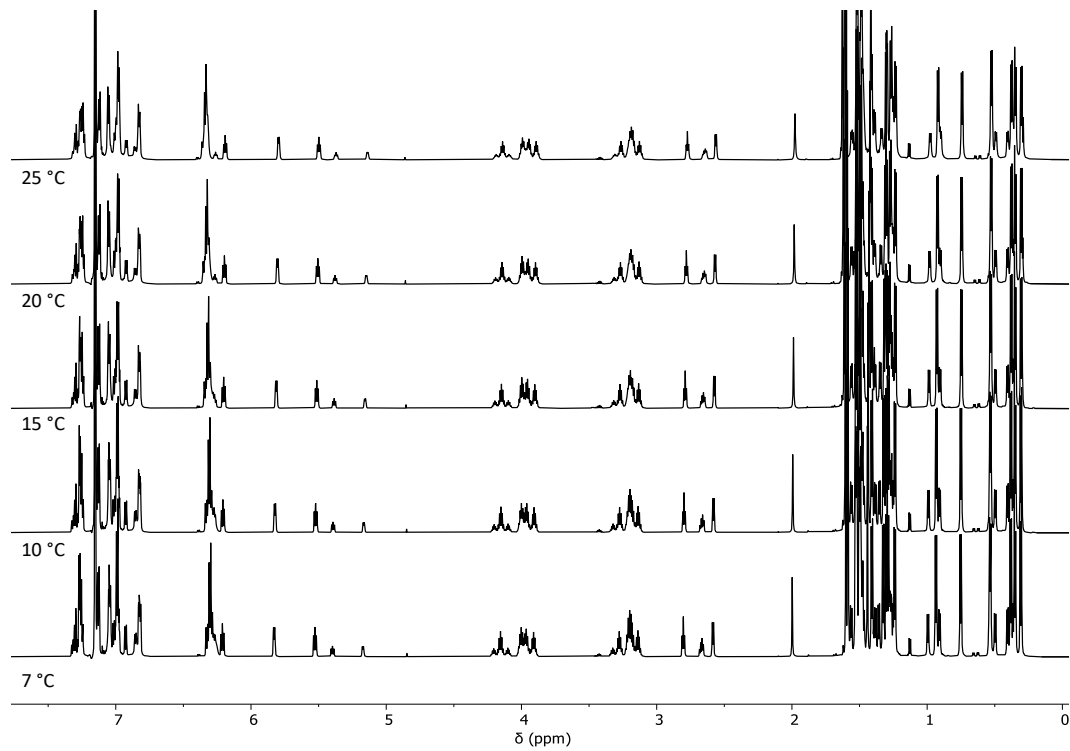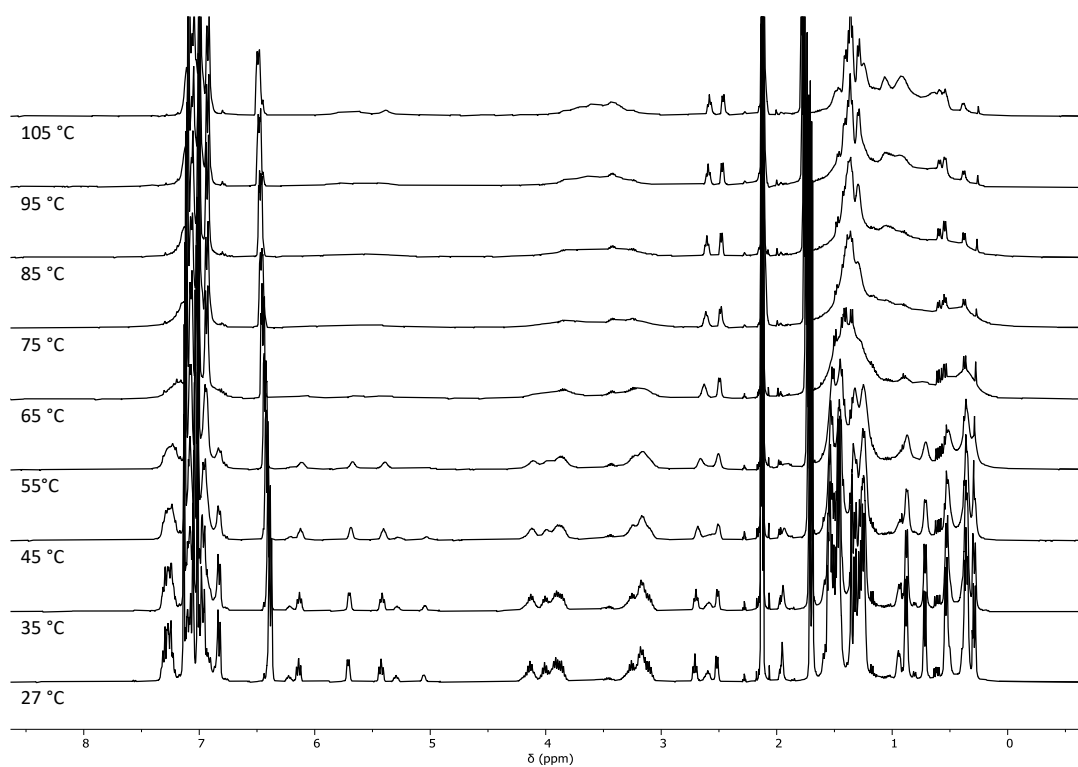**Figure S2:** Comparison of ^{1}H NMR spectra of crude reaction mixtures of **1** and **2** (upfield region)

Figure S3: Ratio of integrations of major (α) and minor (β) diene resonances (1:0.4) in ^{1}H NMR of **2**

Figure S4: EXSY NMR spectrum (diene region, ~5–7 ppm) of **2**

Figure S5: Full EXSY NMR spectrum of **2**

Figure S6: Variable temperature NMR (700 MHz) of **2** in benzene-d_6 from 7-25 °C

**Figure S7:** Variable temperature NMR (400 MHz) of **2** in toluene-d_8 from 27-105 °C
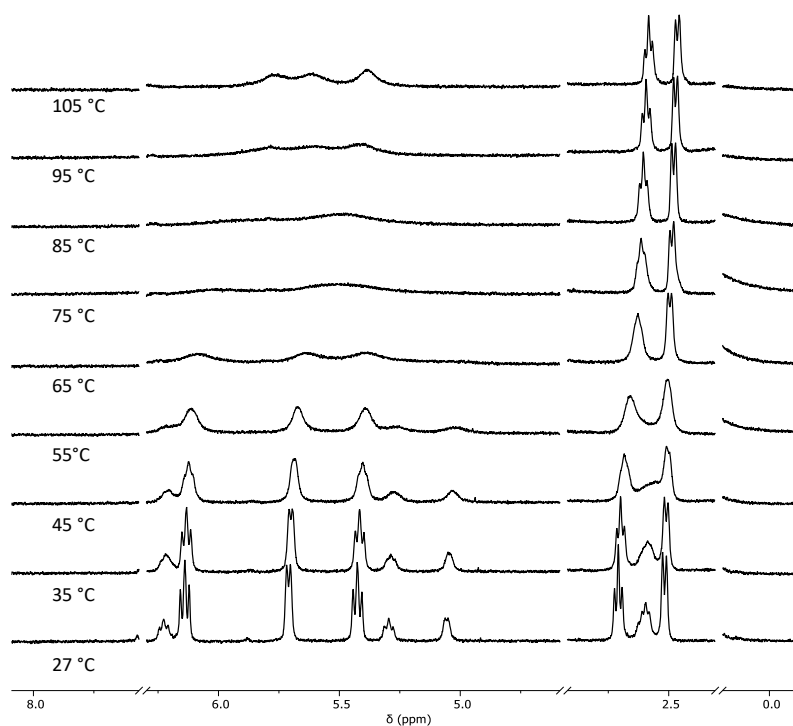
Figure S8: Selected regions (toluene fragment resonances) of variable temperature NMR (400 MHz) of **2** in toluene-d_8 from 27-105 °C
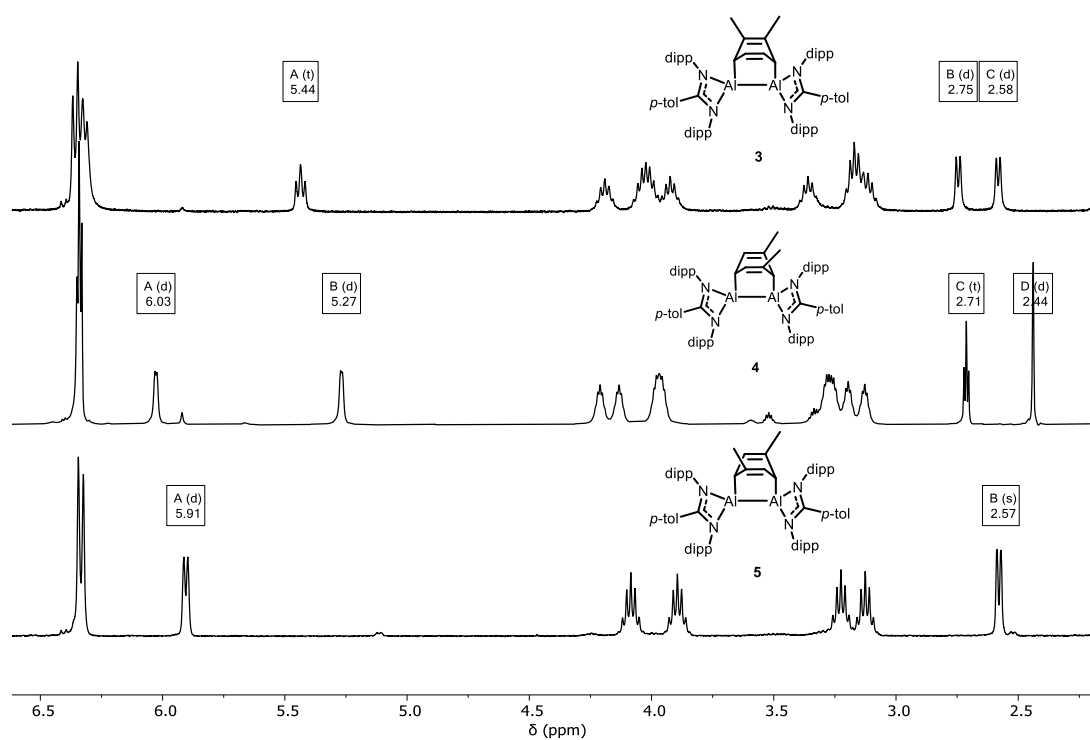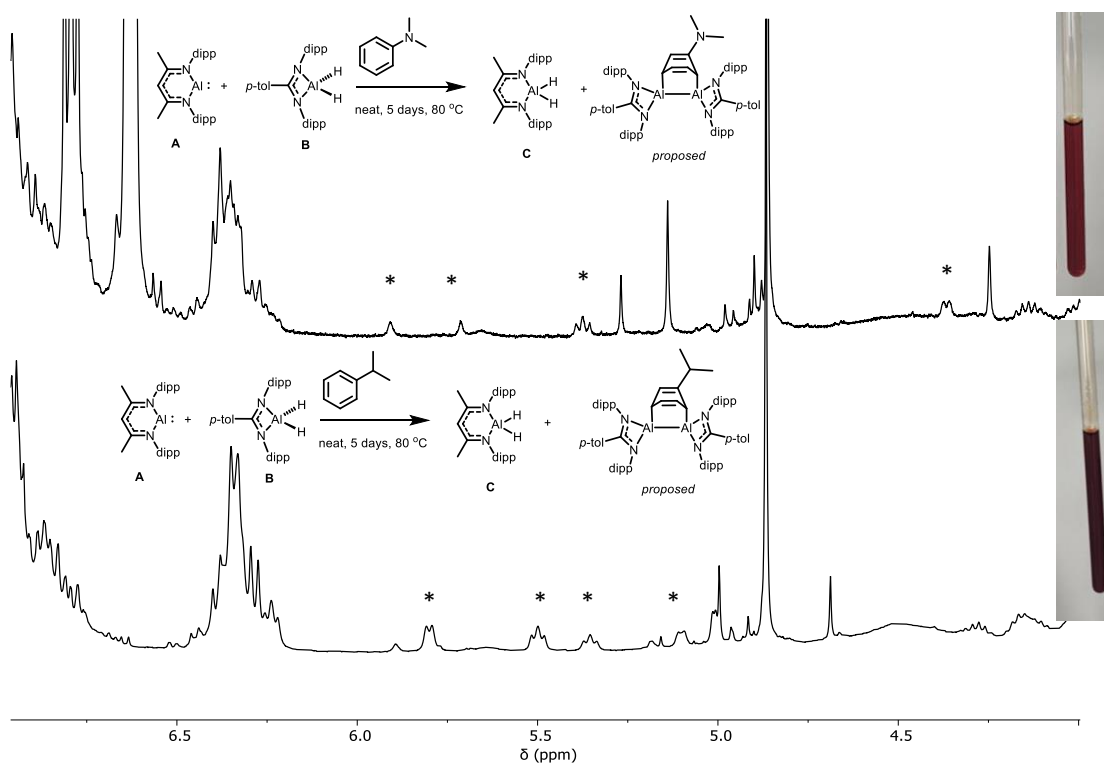
Figure S9: ^{1}H NMR spectra of **3-5**, showing different splitting patterns from methyl substitution on the xylene fragment
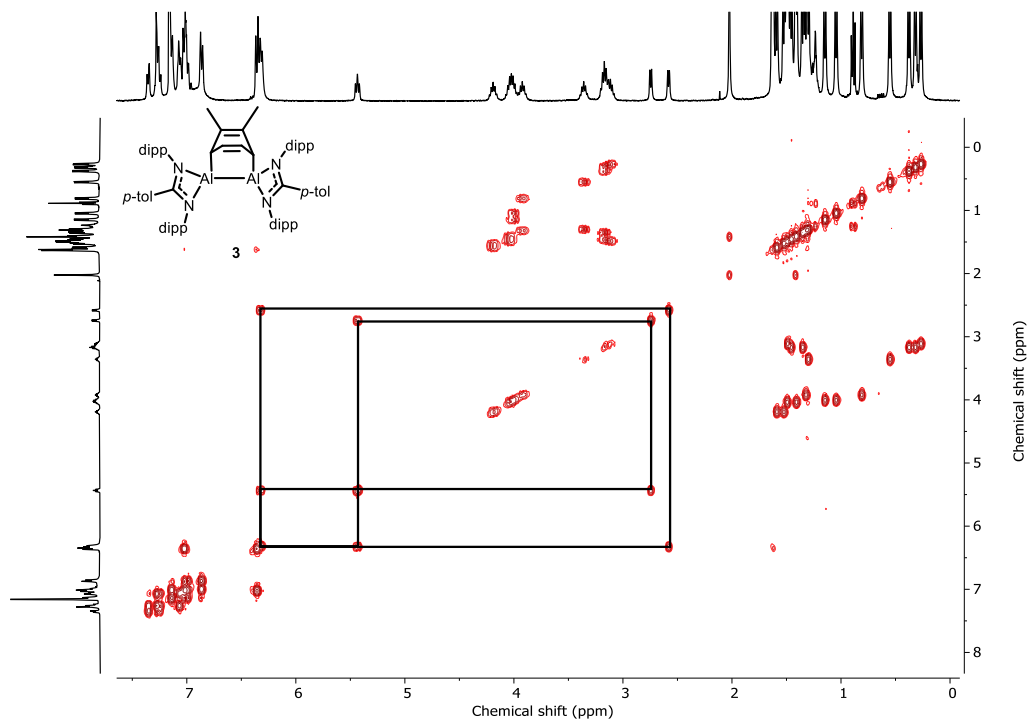

Figure S10: COSY NMR spectrum of **3**, showing cross peaks corresponding to diene protons, indicating obscured resonance at δ_H = 6.33
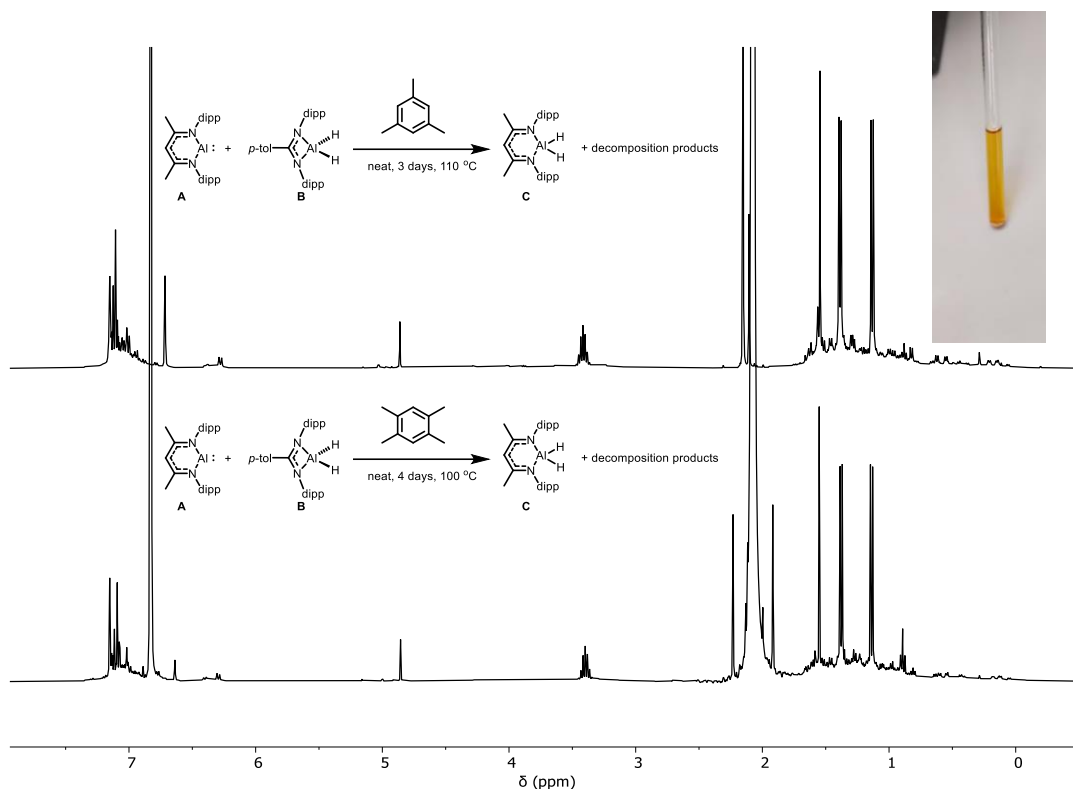
Figure S11: ^{1}H NMR spectra of crude reaction mixtures of **A** and **B** heated in mesitylene (top) and durene (bottom)


Figure S12: ^{1}H NMR spectra (alkene region) of crude reaction mixtures of **A** and **B** in N,N-dimethylaniline (top) and cumene (bottom) – asterisk peaks indicate features indicative of adduct formation, as does the colour
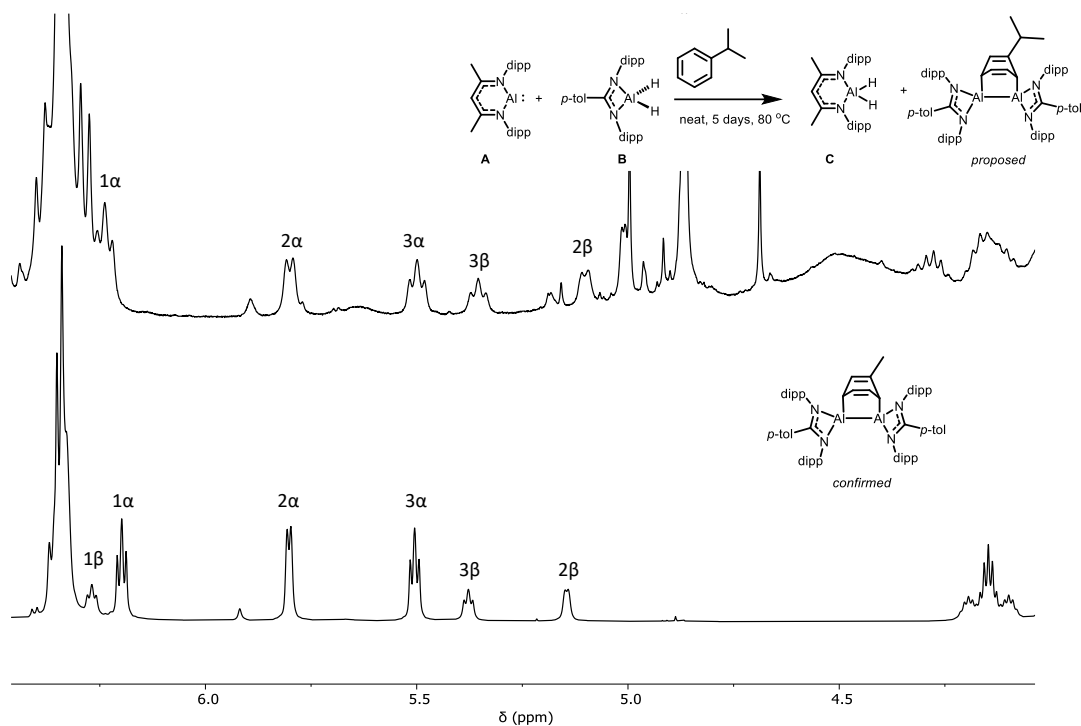
Figure S13: ^{1}H NMR spectra (alkene region) of crude reaction mixture of **A** and **B** in cumene (top) and isolated **2** (bottom)
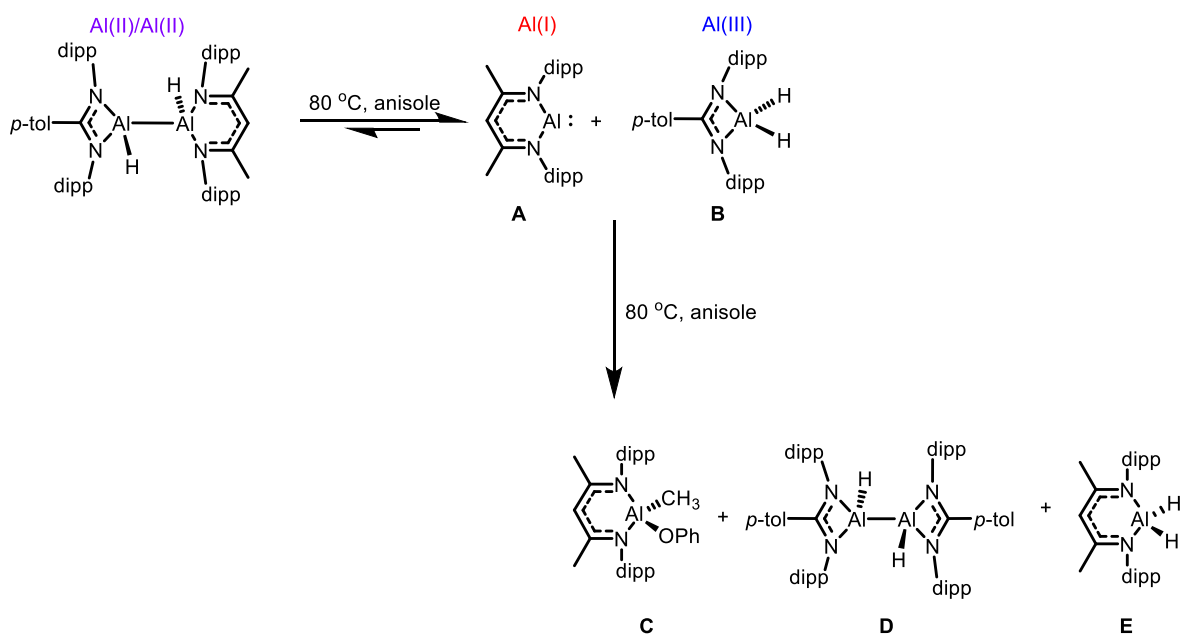

Figure S14: Reaction scheme showing disproportionation of Al(II) dihydrodialane to **A** and **B** (starting materials) in anisole, followed by C-O bond activation of anisole by **A** generating complex **E**[7] (along with **C**[5] and **D**[6])
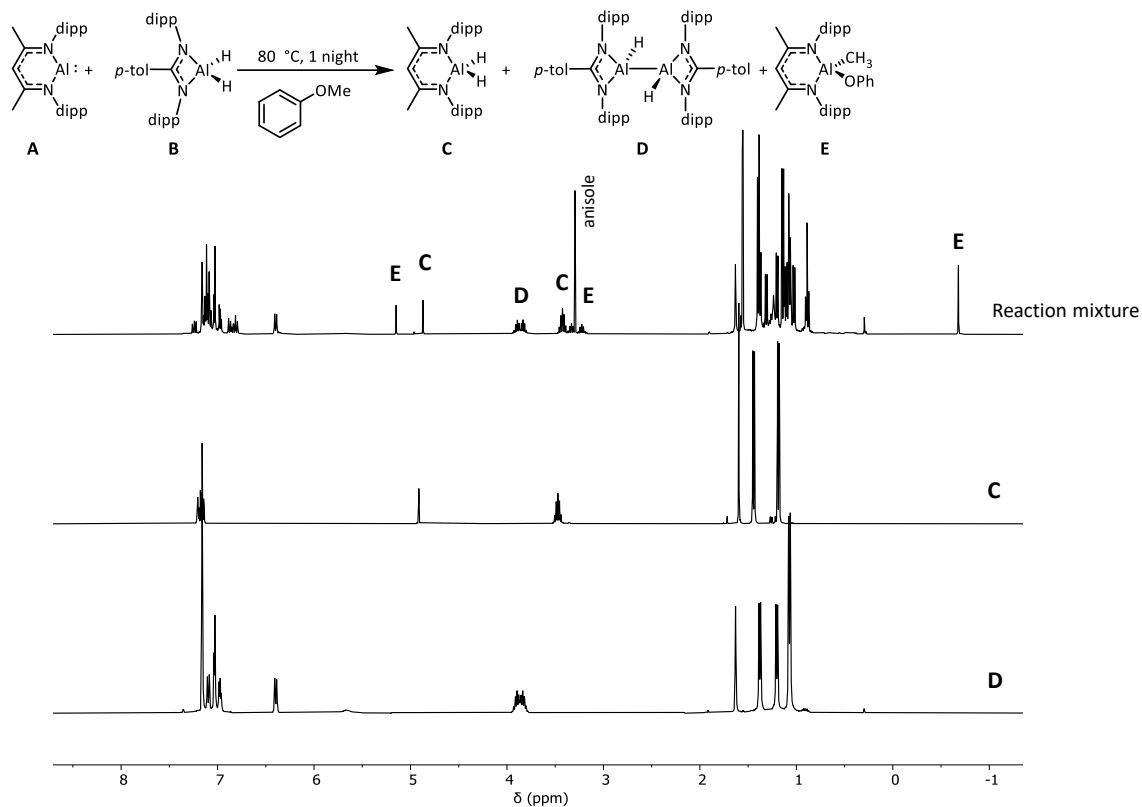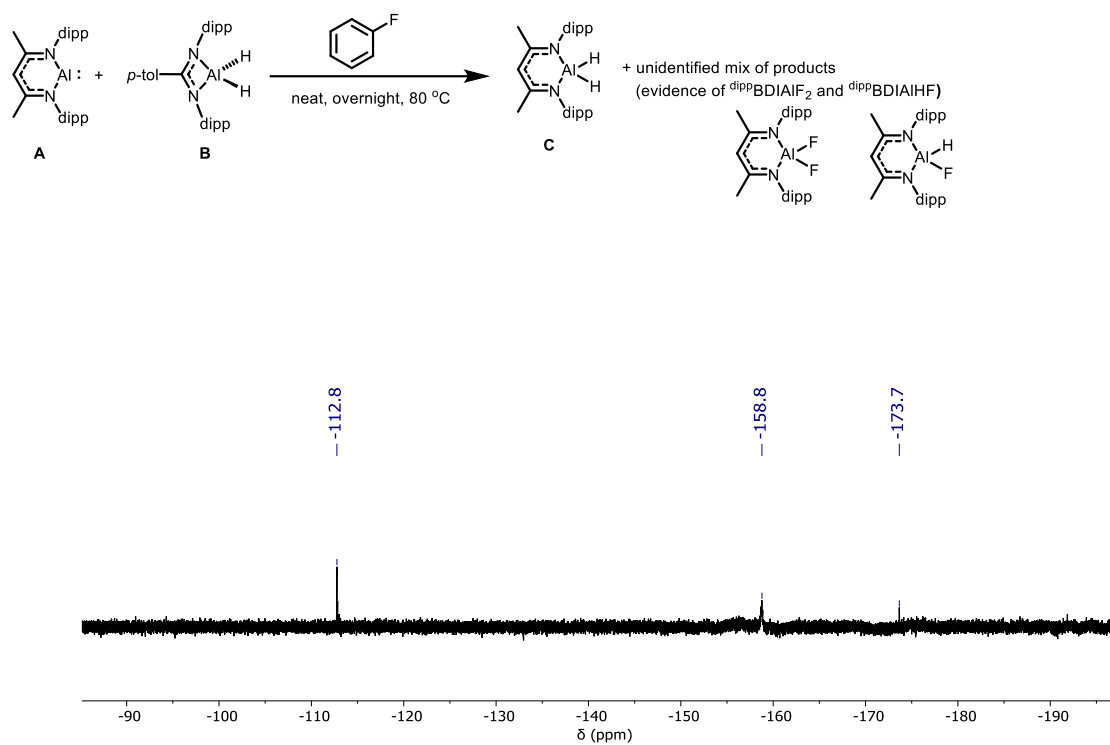
Figure S15: ^{1}H NMR of reaction mixture formed from A and B at 80 °C in anisole, showing formation of 3 previously reported compounds (**C**[5], **D**[6] and **E**[7])
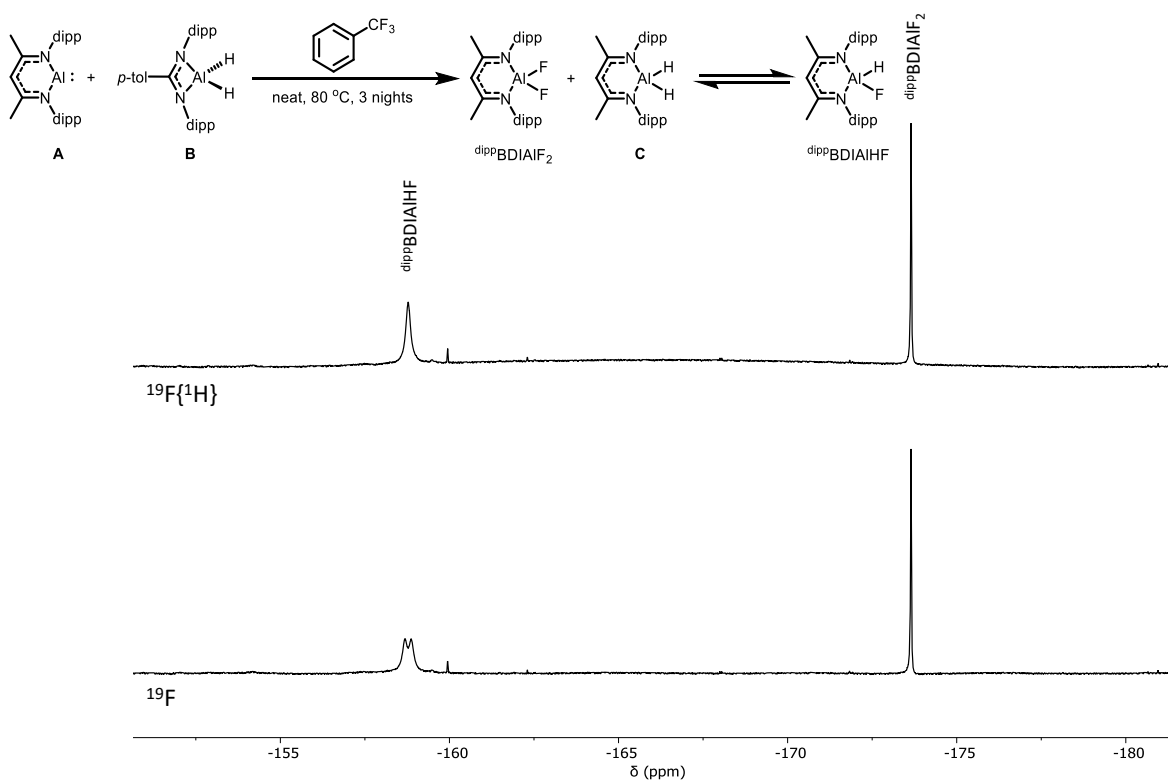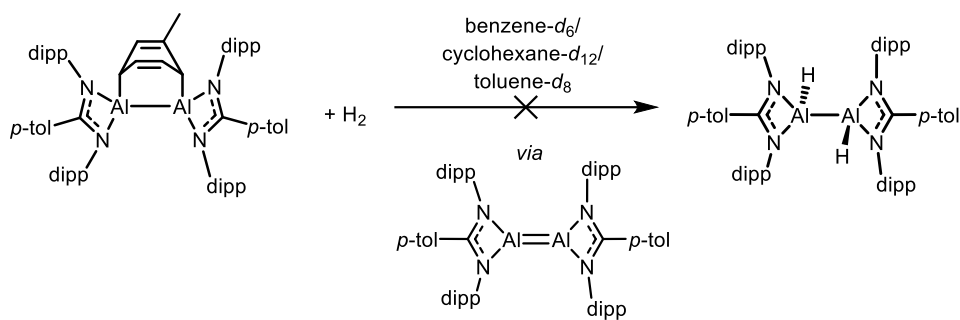

Figure S16: ^{19}F NMR of reaction between **A** and **B** in trifluorotoluene (resonances displayed corresponding to those previously reported)[11]
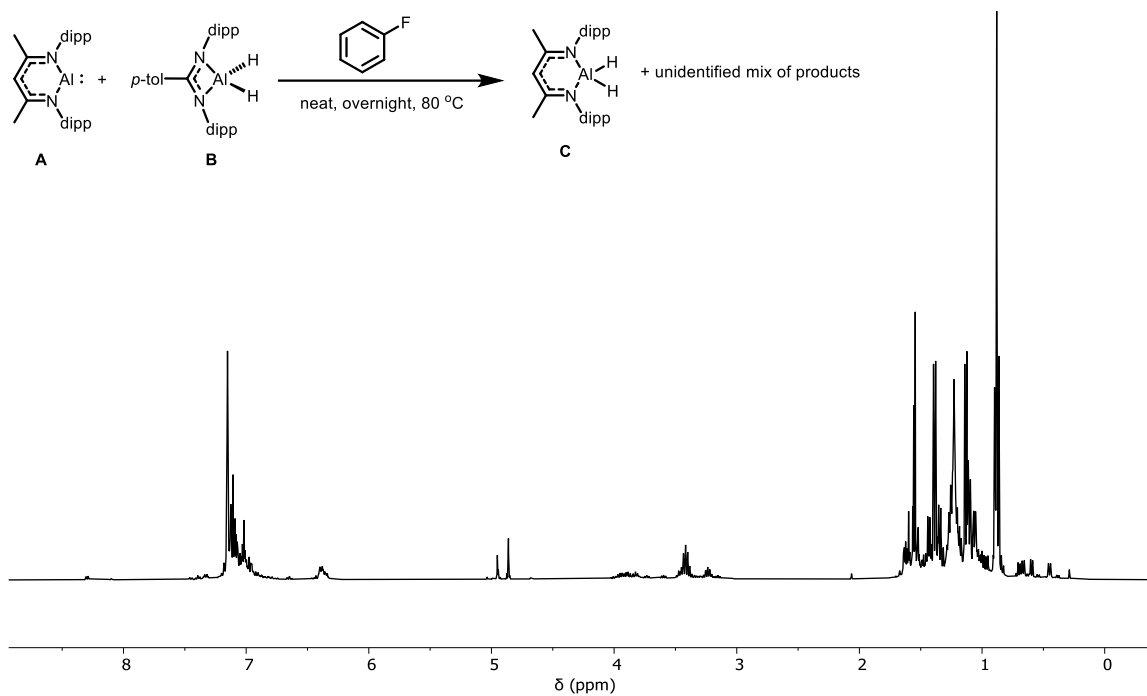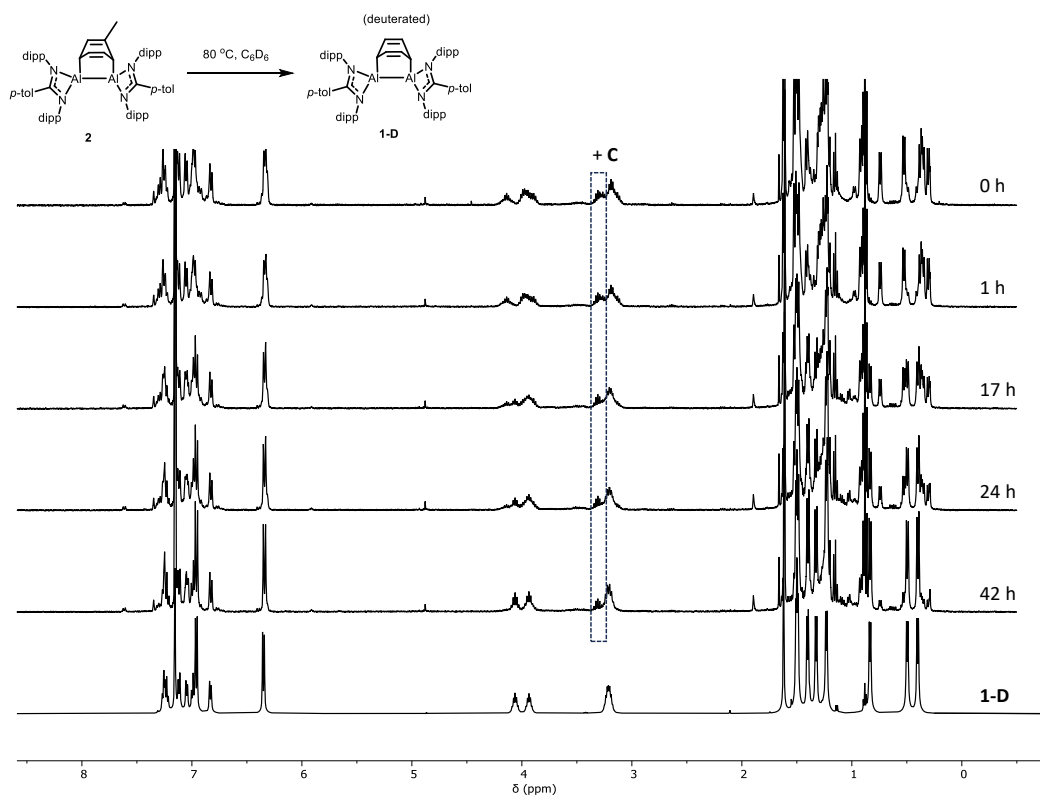
Figure S17: ^{1}H NMR of reaction between **A** and **B** in fluorobenzene

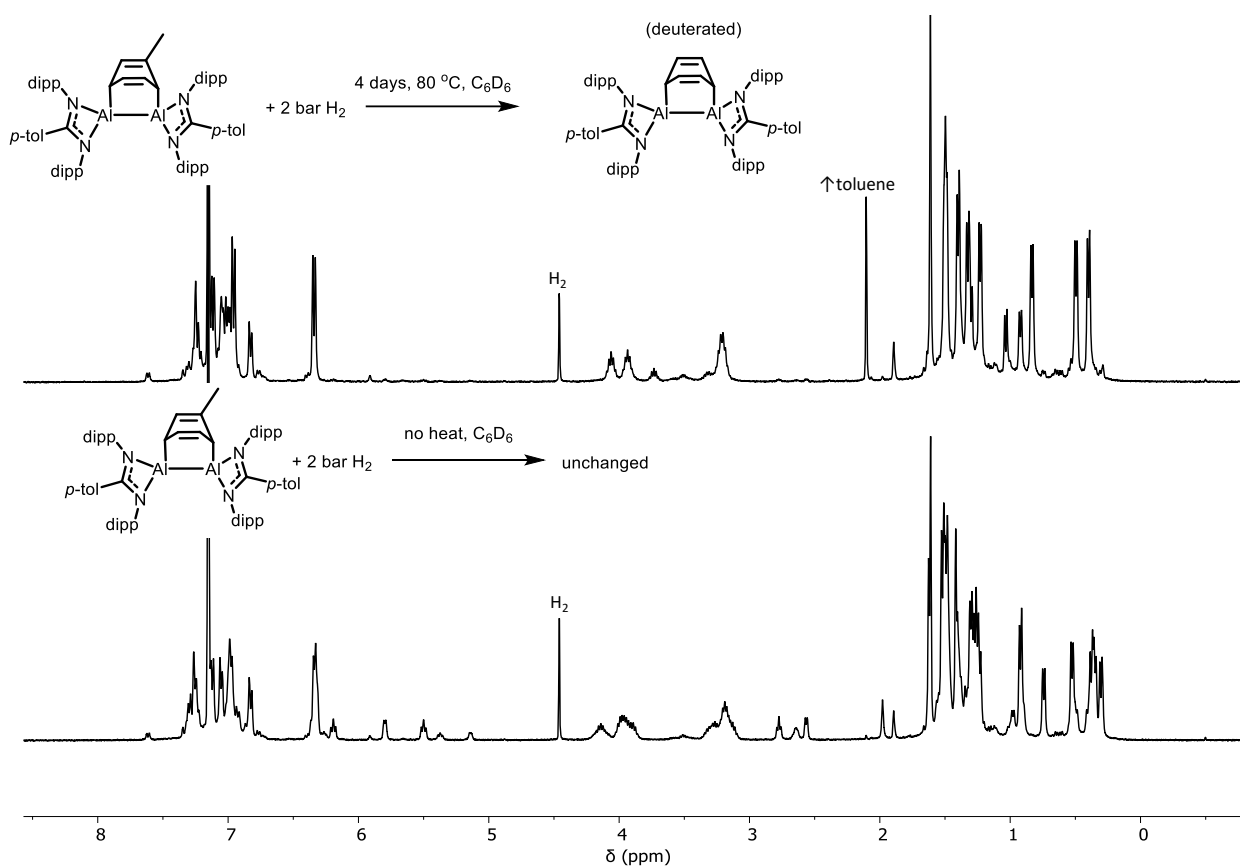**Figure S18:** ^{19}F NMR of reaction between **A** and **B** in fluorobenzene

Figure S19: Proposed reaction scheme between **2** and H_2

Figure S20: ^{1}H NMR of heating **2** at 80 °C in C_6D_6, showing conversion to **1-D** (bottom spectrum) over 42 hours

Figure S21: ^{1}H NMR of reaction between **2** and H$_2$ in C$_6$D$_6$ (bottom), producing **1-D** (top)

4. X-ray crystallographic data

All experiments were performed at 150.15 K using a Cu Kα radiation source (λ = 1.54184 Å). Measurements on compounds **2**, **4** and **5** were made using a twin-source Agilent Oxford Diffraction SuperNova diffractometer with a micro-focus Cu Kα X-ray beam (50 kV, 0.8 mA) and an Atlas CCD detector. Measurements on compound **3** were made using a twin-source Oxford Xcaliubur Gemini diffractometer with a Sapphire 3 CCD plate. Cell refinement, data collection and data reduction for all experiments were performed using Rigaku CrysAlisPro. Using Olex2,[8] the structure was solved with the ShelXT[9] structure solution program using Intrinsic Phasing and refined with the ShelXL[10] refinement package using Least Squares minimisation.
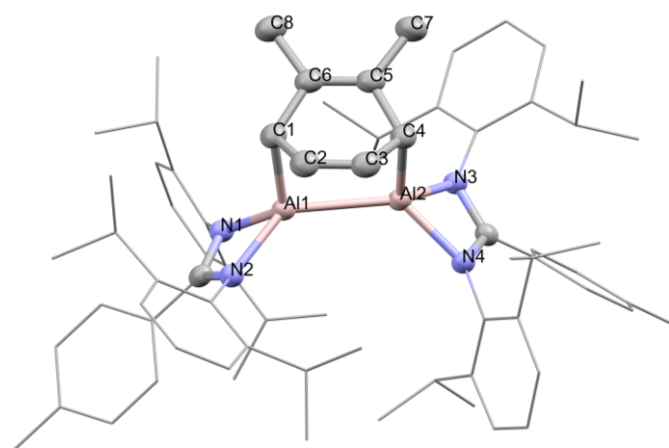
*The X-ray crystal structure of **2***
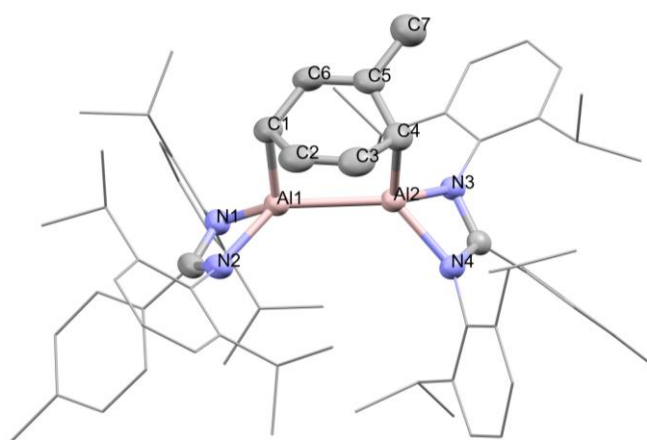
Figure S22: The X-ray crystal structure of **2**. Hydrogen atoms and disorder omitted for clarity, key atoms shown as thermal ellipsoids at 50% probability.

Single crystals of **2** were grown by slow evaporation from hexane solution. **2** was found to crystallise in the P2$_1$/n space group. The unit cell contained 1 hexane molecule per unit cell, which was modelled using a solvent mask (SQUEEZE). Part of the ligand (C22-C28) was disordered over two positions. The methyl group of the toluene fragment (C7) was disordered over two positions with relative occupancies 0.818:0.182.

*Crystal data for **2***: C$_{71}$H$_{90}$Al$_2$N$_4$ (*M* =1053.49 g/mol): monoclinic, space group P2$_1$/n (no. 14), *a* = 15.2755(2) Å, *b* = 20.2100(2) Å, *c* = 24.2085(3) Å, *β* = 105.8240(10)°, *V* = 7190.38(15) Å^3, *Z* = 4, *T* = 150.15 K, μ(Cu Kα) = 0.681 mm^{-1}, *Dcalc* = 1.052 g/cm^3, 49375 reflections measured (7.438° ≤ 2Θ ≤ 154.05°), 14362 unique (*R*$_{int}$ = 0.0383, R$_{sigma}$ = 0.0392) which were used in all calculations. The final *R*$_1$ was 0.0484 (I > 2σ(I)) and *wR*$_2$ was 0.1293 (all data). CCDC deposition number 2365635.

Table S1: Key bond lengths (Å) and bond angles (°) of **2**

Al1-Al2	Al1-N1	Al1-N2	Al2-N3	Al2-Al4	Al1-C1	Al2-C4
2.5520(6)	1.949(1)	1.944(2)	1.944(1)	1.951(1)	2.016(2)	2.021(2)
C1-C2	**C2-C3**	**C3-C4**	**C4-C5**	**C5-C6**	**C1-C6**	**C5-C7**
1.499(3)	1.321(2)	1.510(3)	1.499(3)	1.322(3)	1.500(2)	1.502(3)
N1-Al1-N2	**N3-Al2-N4**	**C1-Al1-Al2**	**C4-Al2-Al1**	**C6-C1-C2**	**C3-C4-C5**	**C6-C5-C7**
68.36(6)	68.332(5)	94.10(6)	93.66(6)	109.6(2)	109.8(2)	121.3(2)

The X-ray crystal structure of 3

Figure S23: The X-ray crystal structure of **3**. Hydrogen atoms and solvent molecules omitted for clarity, key atoms shown as thermal ellipsoids at 50% probability.
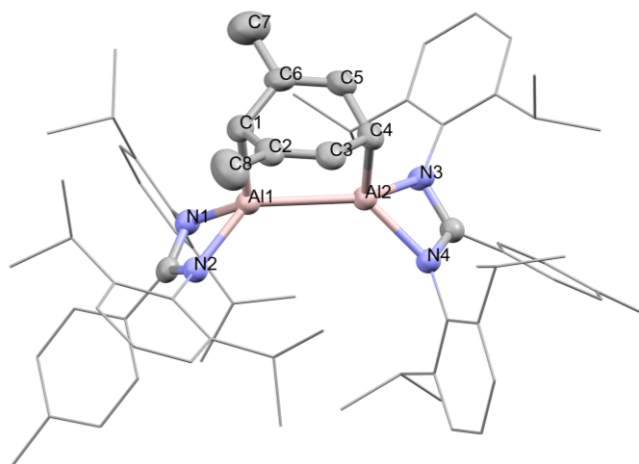
Single crystals of **3** were grown by slow evaporation from toluene solution. **3** was found to crystallise in the P-1 space group. The unit cell contained 1 toluene molecule per unit cell.

*Crystal data for **3**:* $C_{72}H_{92}Al_2N_4 \cdot C_7H_8$ (*M* =1159.58 g/mol): triclinic, space group P-1 (no. 2), a = 13.1124(4) Å, b = 13.4322(4) Å, c = 21.3152(7) Å, α = 75.831(3)°, β = 82.021(3)°, γ = 75.106(3)°, V = 3506.2(2) Å^3, Z = 2, T = 150.15 K, μ(CuKα) = 0.702 mm^{-1}, $Dcalc$ = 1.098 g/cm^3, 24756 reflections measured (6.978° ≤ 2Θ ≤ 144.448°), 13471 unique (R_{int} = 0.0248, R$_{sigma}$ = 0.0365) which were used in all calculations. The final R_1 was 0.0438 (I > 2σ(I)) and wR_2 was 0.1235 (all data). CCDC deposition number 2365636.

Table S2: Key bond lengths (Å) and bond angles (°) of **3**

Al1-Al2	Al1-N1	Al1-N2	Al2-N3	Al2-Al4	Al1-C1	Al2-C4	
2.5485(7)	1.959(1)	1.948(2)	1.942(2)	1.957(1)	2.017(1)	2.023(1)	
C1-C2	**C2-C3**	**C3-C4**	**C4-C5**	**C5-C6**	**C1-C6**	**C5-C7**	**C6-C8**
1.501(2)	1.343(3)	1.501(3)	1.519(2)	1.341(3)	1.509(3)	1.506(3)	1.509(2)
N1-Al1-N2	**N3-Al2-N4**	**C1-Al1-Al2**	**C4-Al2-Al1**	**C6-C1-C2**	**C3-C4-C5**	**C6-C5-C7**	**C5-C6-C8**
68.35(6)	68.14(6)	95.34(5)	93.19(5)	110.1(1)	110.0(1)	124.8(2)	125.0(2)

*The X-ray crystal structure of **4***

Figure S24: The X-ray crystal structure of **4**. Hydrogen atoms and disorder omitted for clarity, key atoms shown as thermal ellipsoids at 50% probability.
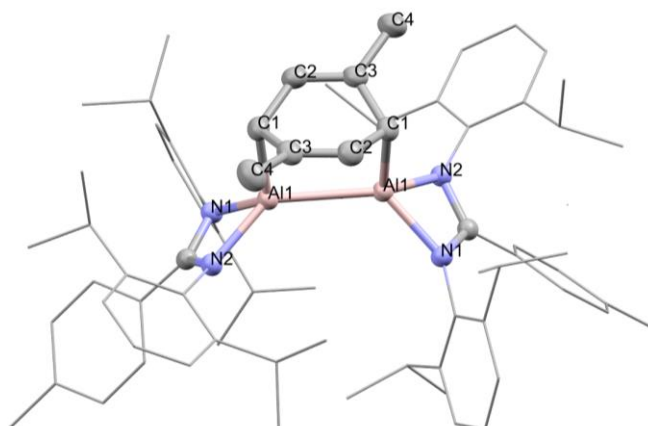
Single crystals of **4** were grown by slow evaporation from hexane solution. **4** was found to crystallise in the I2/a space group. The unit cell contained 1 hexane molecule per unit cell, which was modelled using a solvent mask (SQUEEZE). Two parts of the ligand (C17-C19 and C20-C26) were disordered over two positions. The methyl groups on the *m*-xylene fragment (C7 and C8) were disordered over two positions with relative occupancies 0.737:0.262.

Crystal data for **4**: $C_{72}H_{92}Al_2N_4$ (*M* =1067.52 g/mol): monoclinic, space group I2/a (no. 15), *a* = 16.5835(2) Å, *b* = 16.8300(2) Å, *c* = 51.4307(5) Å, *β* = 96.7230(10)°, *V* = 14255.6(3) Å^3, *Z* = 8, *T* = 150.15 K, μ(CuKα) = 0.685 mm^{-1}, *Dcalc* = 1.072 g/cm^3, 48283 reflections measured (7.386° ≤ 2Θ ≤ 154.388°), 14327 unique (R_{int} = 0.0711, R_{sigma} = 0.0614) which were used in all calculations. The final R_1 was 0.0550 (I > 2σ(I)) and *wR*$_2$ was 0.1488 (all data). CCDC deposition number 2365637.

Table S3: Key bond lengths (Å) and bond angles (°) of **4**

Al1-Al2	Al1-N1	Al1-N2	Al2-N3	Al2-Al4	Al1-C1	Al2-C4	
2.561(1)	1.973(2)	1.937(1)	1.935(2)	1.969(1)	2.019(2)	2.009(2)	
C1-C2	**C2-C3**	**C3-C4**	**C4-C5**	**C5-C6**	**C1-C6**	**C6-C7**	**C2-C8**
1.509(3)	1.337(2)	1.501(3)	1.502(3)	1.342(3)	1.506(3)	1.496(4)	1.508(3)
N1-Al1-N2	**N3-Al2-N4**	**C1-Al1-Al2**	**C4-Al2-Al1**	**C6-C1-C2**	**C3-C4-C5**	**C5-C6-C7**	**C3-C2-C8**
67.98(6)	68.21(6)	93.94(6)	93.76(6)	109.8(2)	109.7(2)	122.9(2)	120.7(2)

*The X-ray crystal structure of **5***

Figure S25: The X-ray crystal structure of **5**. Hydrogen atoms and solvent molecules omitted for clarity, key atoms shown as thermal ellipsoids at 50% probability.

Single crystals of **5** were grown by slow evaporation from hexane solution. **5** was found to crystallise in the C2/c space group. The unit cell contained 1 hexane molecule per unit cell, which was disordered over two positions. There was a plane of symmetry through the centre, with half the molecule in the unit cell.

Crystal data for **5**: $C_{72}H_{92}Al_2N_4 \cdot C_6H_{14}$ (M =1153.70 g/mol): monoclinic, space group C2/c (no. 15), a = 22.1421(3) Å, b = 16.4913(2) Å, c = 19.8962(2) Å, β = 103.4350(10)°, V = 7066.32(15) Å^3, Z = 4, T = 150.15 K, μ(Cu Kα) = 0.691 mm^{-1}, $Dcalc$ = 1.081 g/cm^3, 84705 reflections measured (6.75° ≤ 2Θ ≤ 160.09°), 7463 unique (R_{int} = 0.0514, R_{sigma} = 0.0244) which were used in all calculations. The final R_1 was 0.0431 (I > 2σ(I)) and wR_2 was 0.1258 (all data). CCDC deposition number 2365638.

Table S4: Key bond lengths (Å) and bond angles (°) of **4**

| Al1-Al1	Al1-N1	Al1-N2	Al1-C1
2.5592(7)	1.953(1)	1.955(1)	2.016(2)
C1-C2	**C2-C3**	**C3-C1**	**C3-C4**
1.501(2)	1.343(2)	1.509(2)	1.502(2)
N1-Al1-N2	**C1-Al1-Al1**	**C2-C1-C3**	**C2-C3-C4**
68.22(5)	94.12(5)	109.5(1)	122.9(1)

5. Computational Details

5.1 Computational Methods

DFT calculations were run using Gaussian 09. Al centres were described with Stuttgart SDDAll RECPs and associated basis sets and the 6-31G** basis sets were used for all other atoms.[11–13]The functions ωB97X, M062X and M06L were investigated.

Geometry optimisation calculations were performed without symmetry constraints. Frequency analyses for all stationary points were performed to confirm their nature of the structures as either minima (no imaginary frequency) or transition states (only one imaginary frequency). Free energies reported within the main text are corrected for the effects of benzene solvent (ε=2.2706) using the using the polarizable continuum model (PCM).[14] In addition, single point dispersion corrections were applied to the ωB97X optimised geometries (dispersion corrected ωB97X-D functional).[15] Intrinsic Reaction Coordinate (IRC) calculations followed by full geometry optimisations on final points were used to connect transition states and minima located on the Potential Energy Surface.

The graphical user interface used to visualise the various properties of the intermediates was GaussView 5.0.8. Natural Bond Orbital analysis was carried out in NBO 6.0.[16,17] QTAIM calculations were performed using the AIMAll sotware.[18]

5.2 Functional Testing

A range of different functionals were investigated. The reaction between **Al.Al** and benzene, toluene and mesitylene was used to benchmark calculations against experimental observation. The M06L functional was found to best describe experimental results. Looking at the free energy values for the reaction of Al.Al and mesitylene, only the M06L provides numbers which corroborate the fact the dialumene-mesitylene adduct is not formed experimentally. Otherwise, free energy values for transition states and products were relatively subtle without definitive explanation of reactivity. Calculated reactions pathways in the manuscript using the full ligand system are therefore presented using the M06L functional.
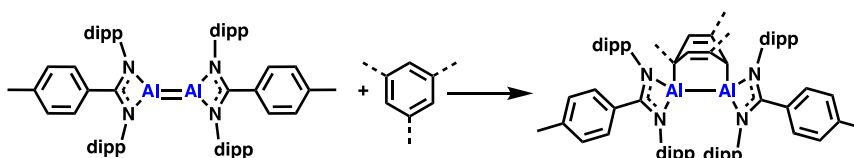
Table S5: Relative free energies and enthalpies (kcal mol^{-1}) of the reaction of **Al.Al** with benzene, toluene and mesitylene using specified density functionals. All values single point corrected for solvent (except entry 1). ωB97XD includes uses a single point D2 correction.

Functional		ωB97X	ωB97XD	M062X	M06L
Benzene	**ΔH**	-33.9	-42.5	-36.4	-28.3
	ΔG	-14.2	-22.8	-18.0	**-9.7**
Toluene	**ΔH**	-35.6	-45.8	-39.1	-30.4
	ΔG	-13.8	-24.0	-18.9	**-9.4**
Mesitylene	**ΔH**	-30.1	-43.6	-37.7	-28.3
	ΔG	-2.4	-16.0	-12.5	**-3.0**

5.3 DFT analysis of Al.Al
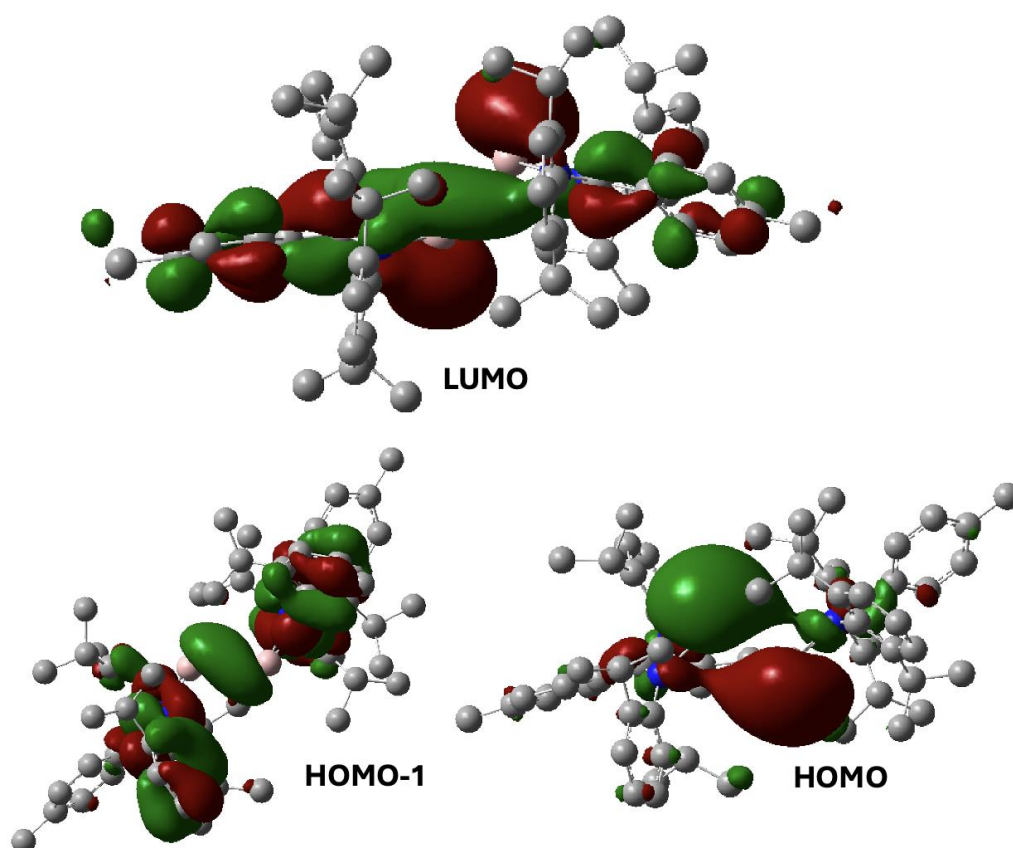
**Figure S26:** Calculated frontier molecular orbitals of **Al.Al**
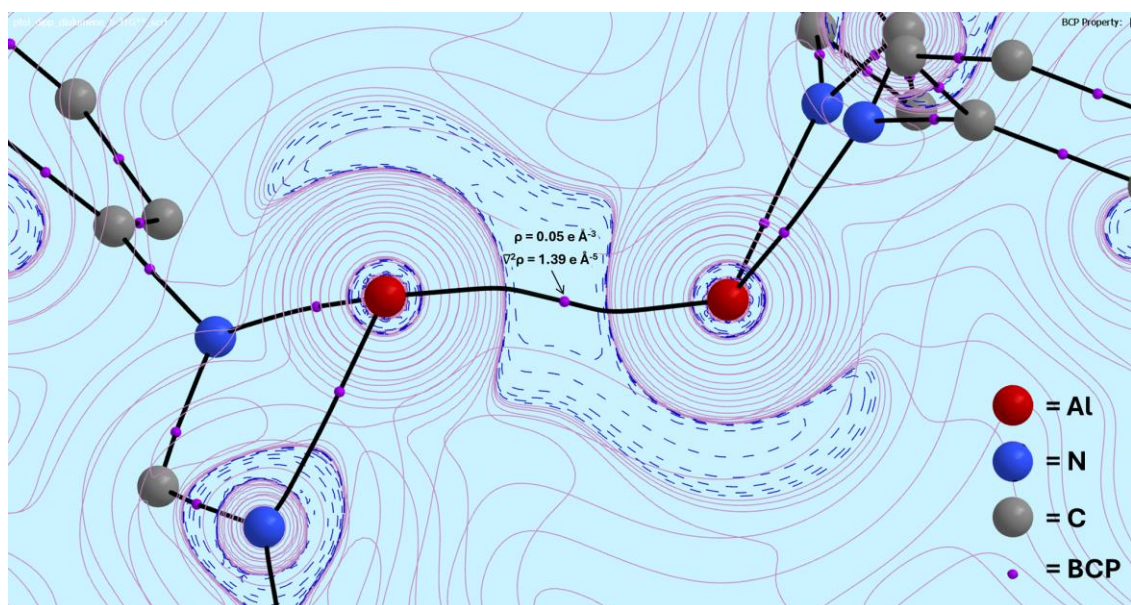
Figure S27: Electron density plot along the Al-Al bond, showing ρ in pink and Laplacian ($\nabla^2\rho$) in blue, outlining areas of charge concentration and depletion. Bond paths in black and bond critical points (bcp) in purple.

5.4 Free energy profiles and transition states calculated using a truncated ligand system
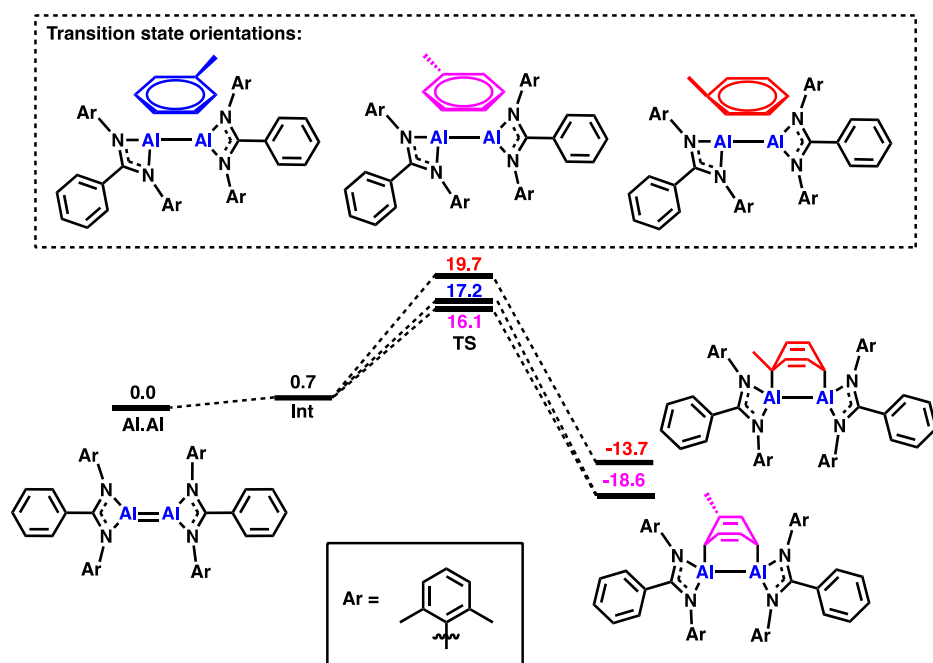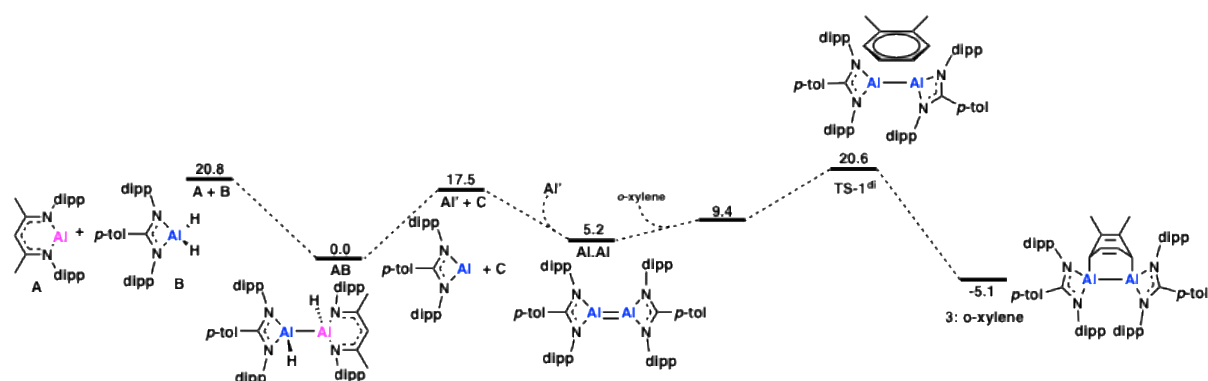

Figure S28: Calculated pathways for the reaction of **Al.Al** with toluene with different possible transition state orientations; Gibbs free energies in kcal mol^{-1}. ωB97XD, Al (SDDAll), C H N (6-31G**) + ΔE$_{solv}$ (PCM, benzene).
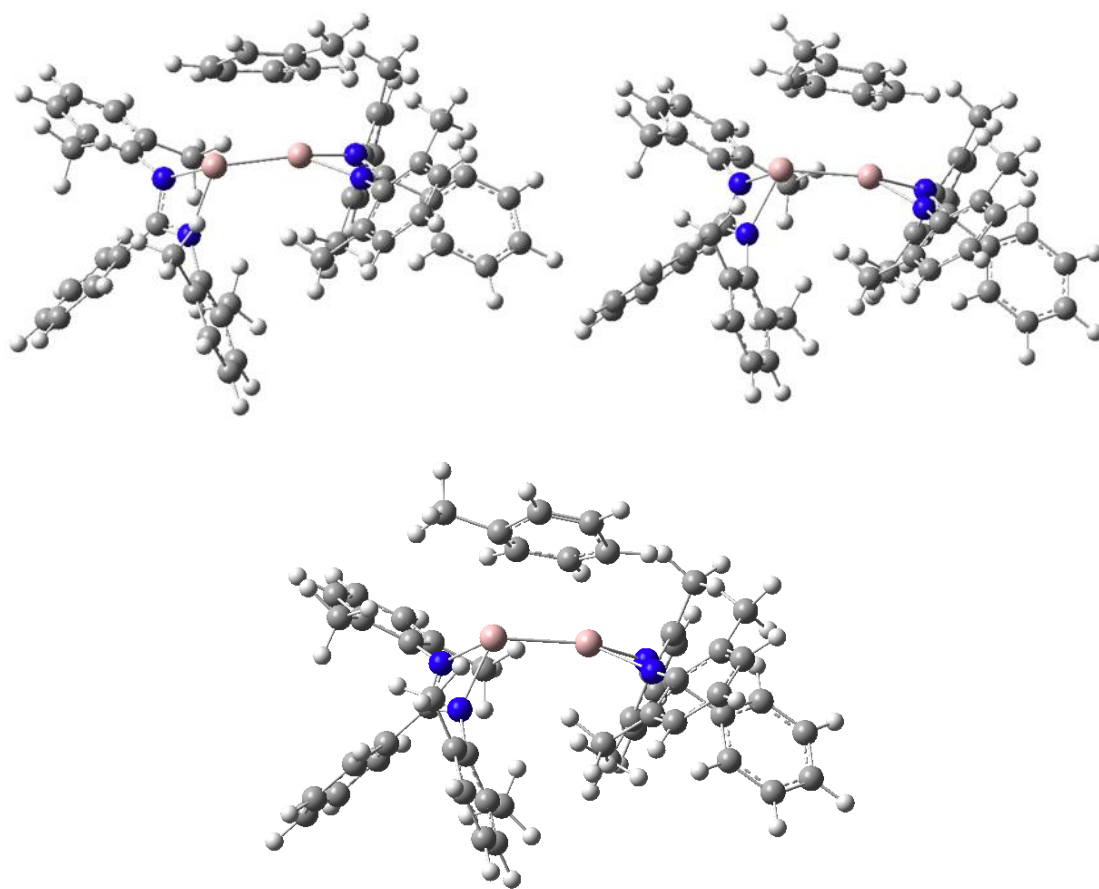
Figure S29: Transition states for three possible approaches of toluene to a dialumene.

5.5 Transition states using the full ligand system

Figure S30: Calculated pathways for the reaction of **Al.Al** with o-xylene. Gibbs free energies in kcal mol^{-1}. ωB97XD, Al (SDDAll), C H N (6-31G**) + ΔE$_{solv}$ (PCM, benzene).
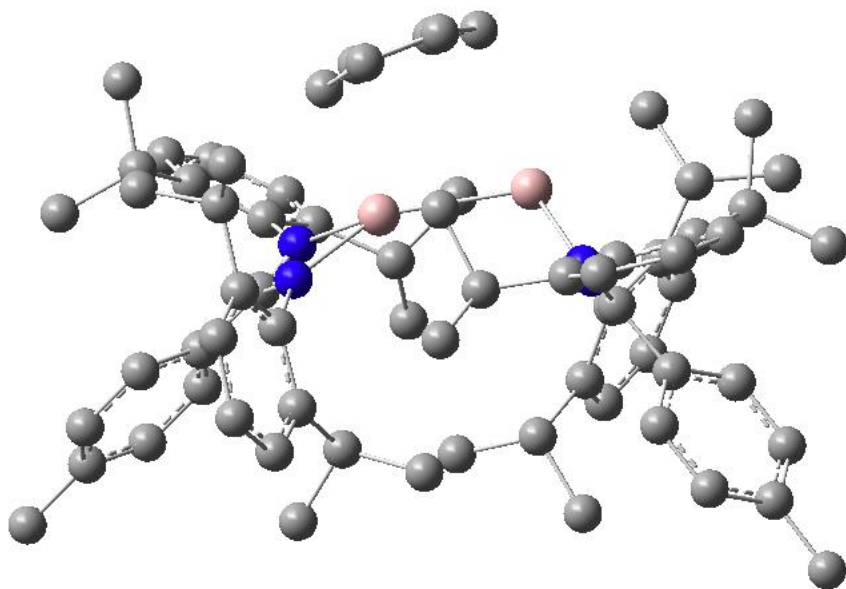
Figure S31: Transition state for the reaction of **Al.Al** and benzene (**TS-1^{di} benzene**). H atoms have been omitted for clarity.
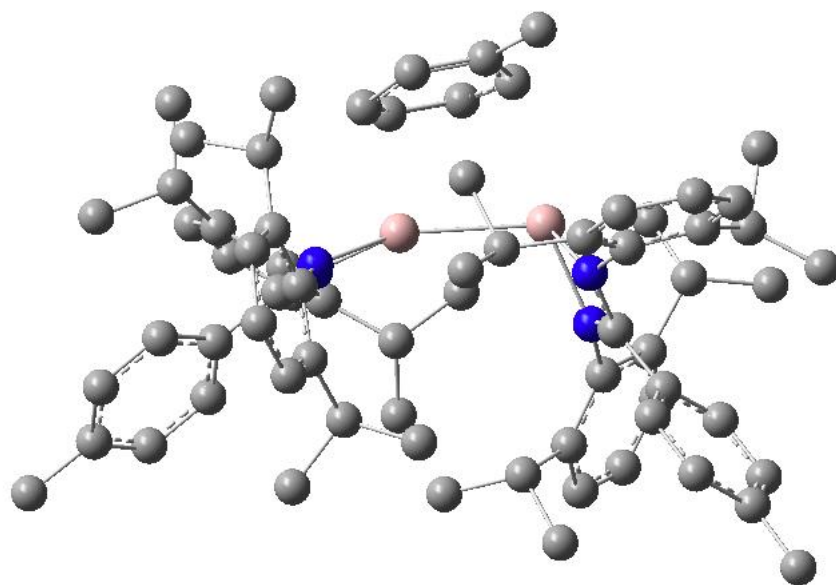
Figure S32: Transition state for the reaction of **Al.Al** and toluene (**TS-1^{di} toluene**). H atoms have been omitted for clarity.
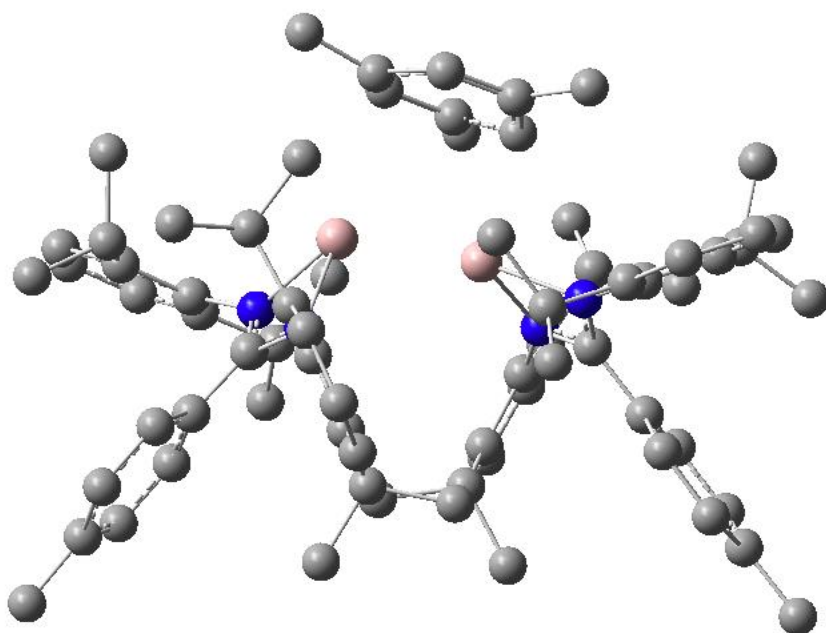
Figure S33: Transition state for the reaction of **Al.Al** and mesitylene (**TS-1^{di} mesitylene**). H atoms have been omitted for clarity.
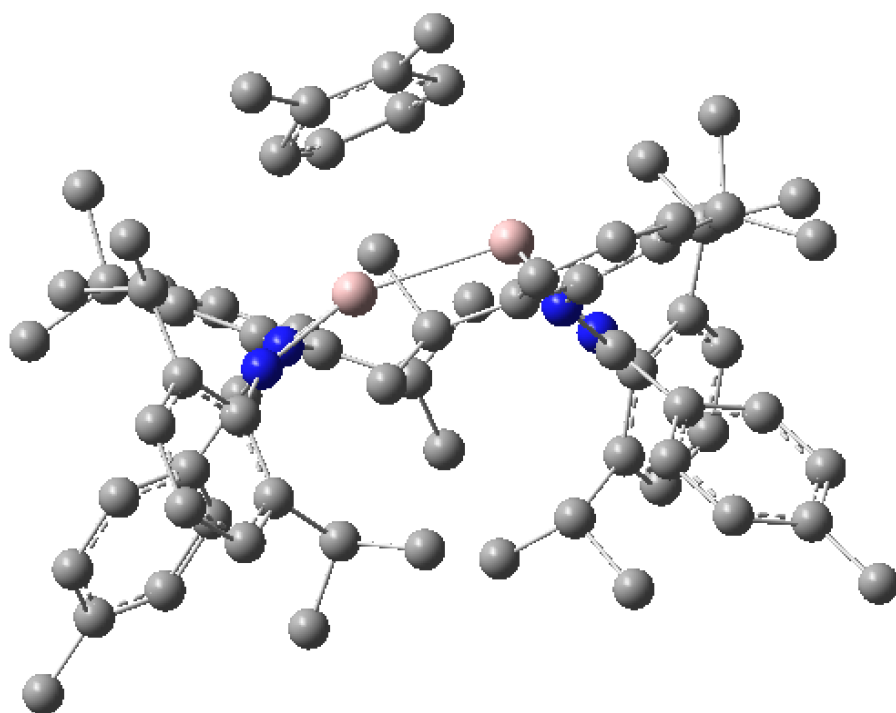
Figure S34: Transition state for the reaction of **Al.Al** and o-xylene (**TS-1**[di] **o-xylene**). H atoms have been omitted for clarity.

6. Multinuclear NMR Data

^{1}H NMR (400 MHz), benzene-d_6, 298 K
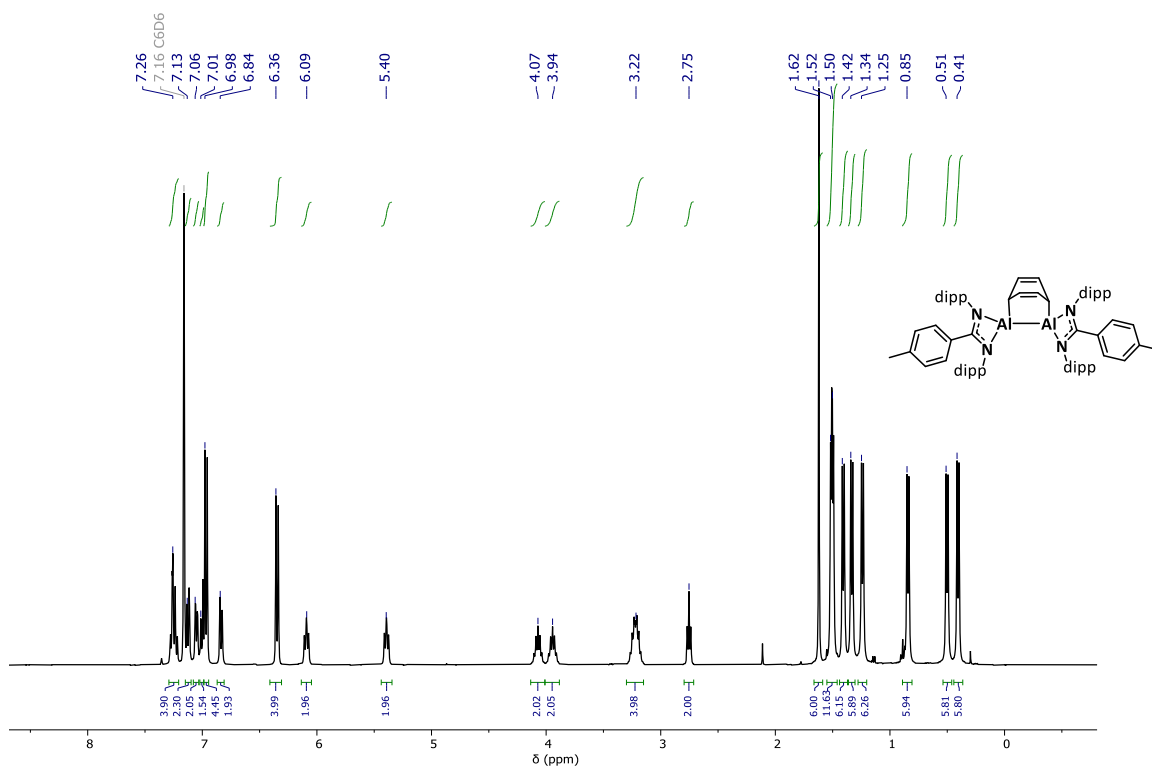
Figure S35: ^{1}H NMR spectrum of compound **1**

^{13}C{^{1}H} NMR (101 MHz), benzene-d_6, 298 K
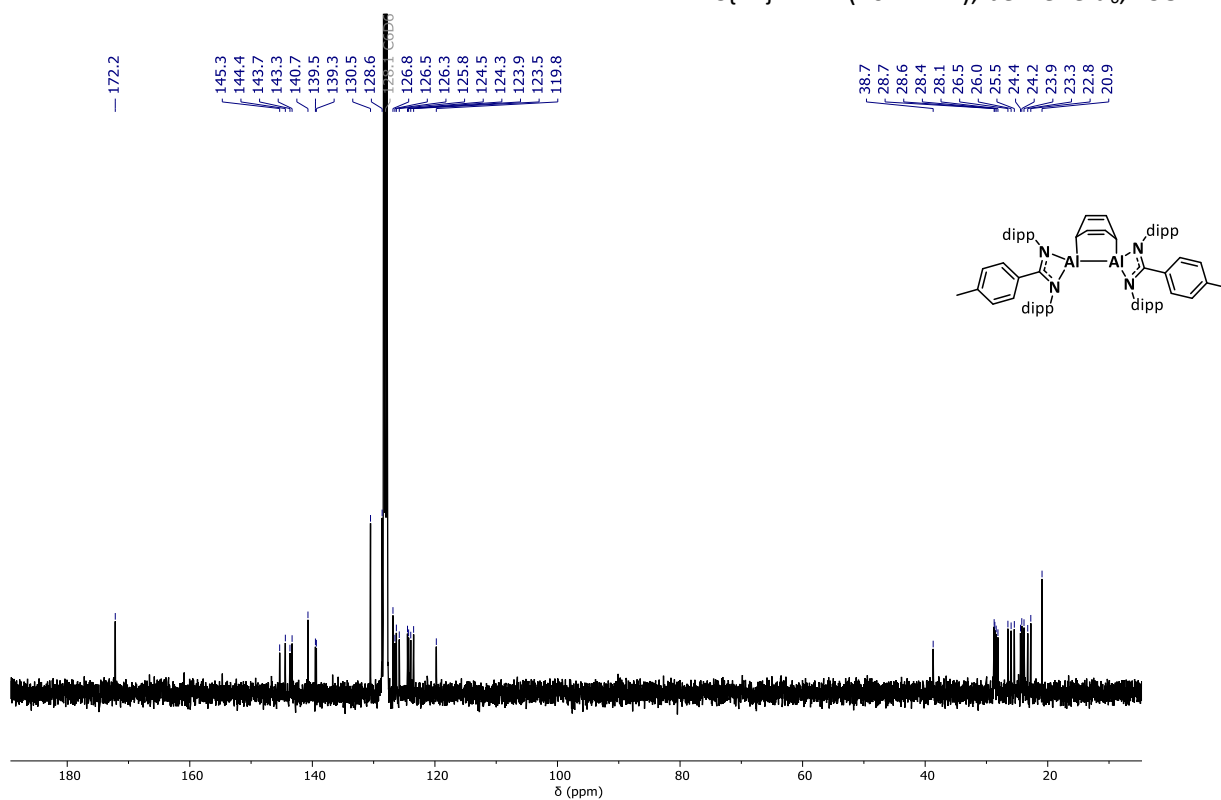
Figure S36: ^{13}C{^{1}H} NMR spectrum of compound **1**
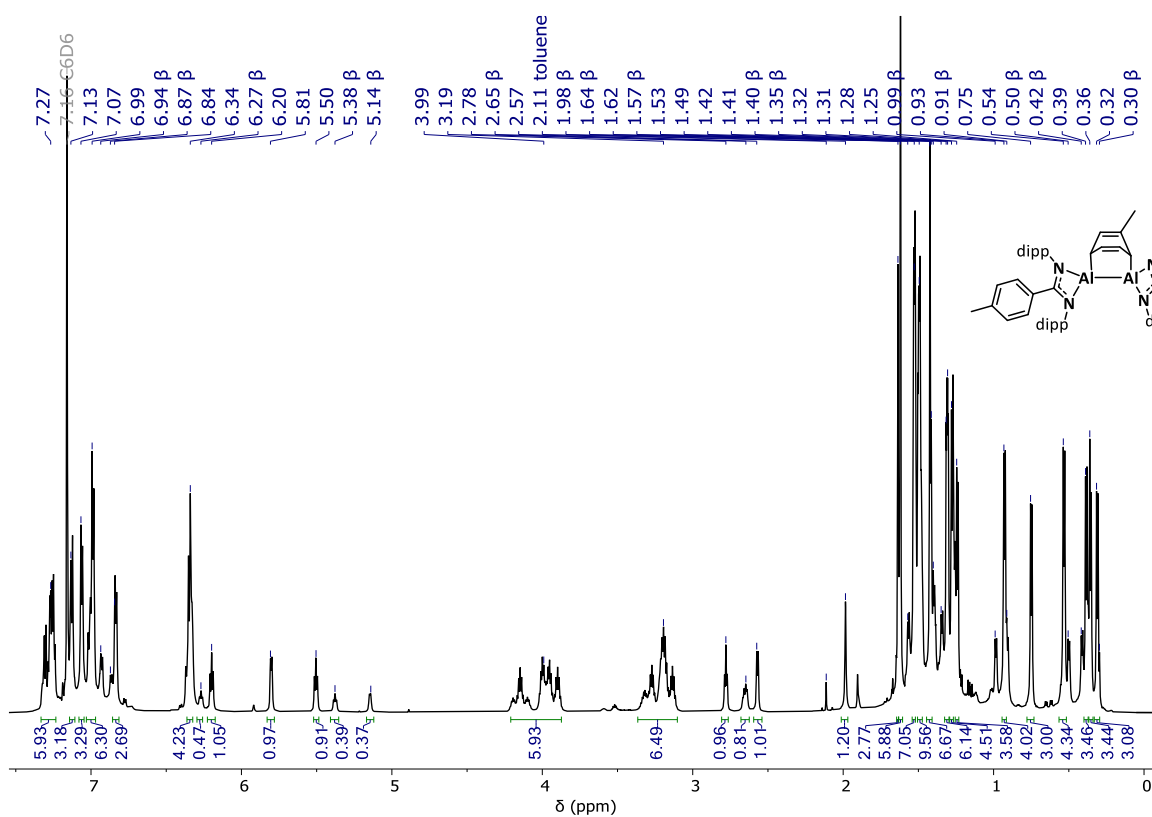
Figure S37: ^{1}H NMR spectrum of compound **2**
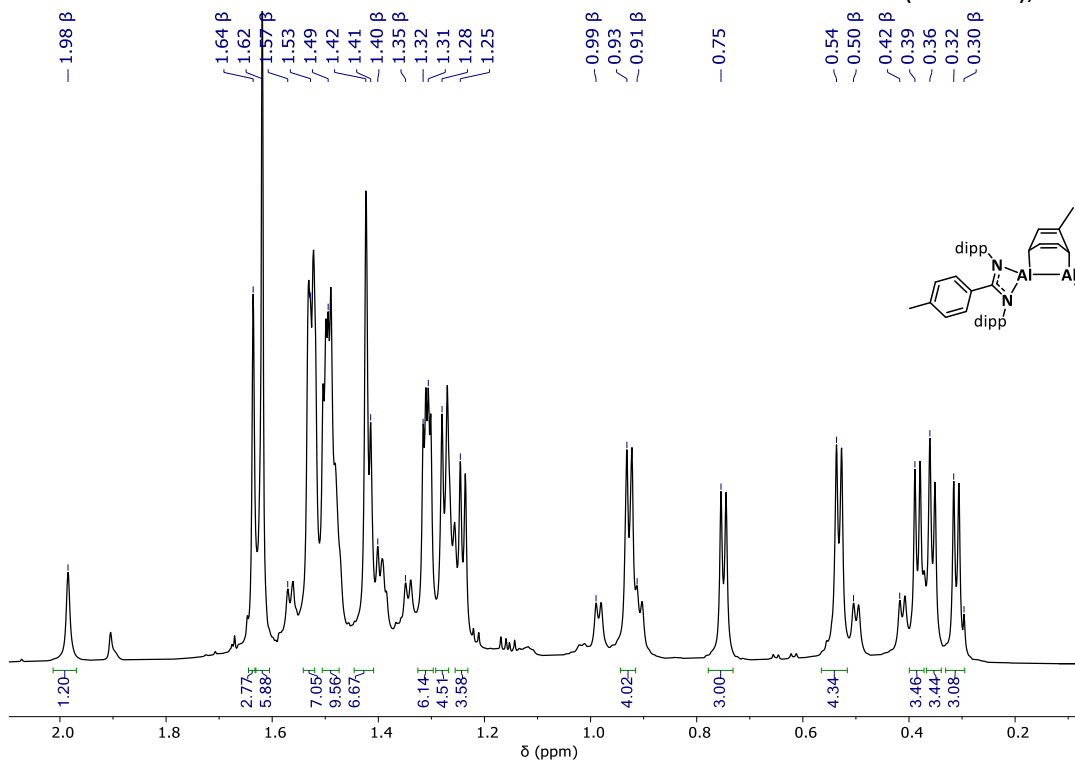
Figure S38: 'Low alkyl region' (0-2 ppm) of ^{1}H NMR spectrum of compound **2**
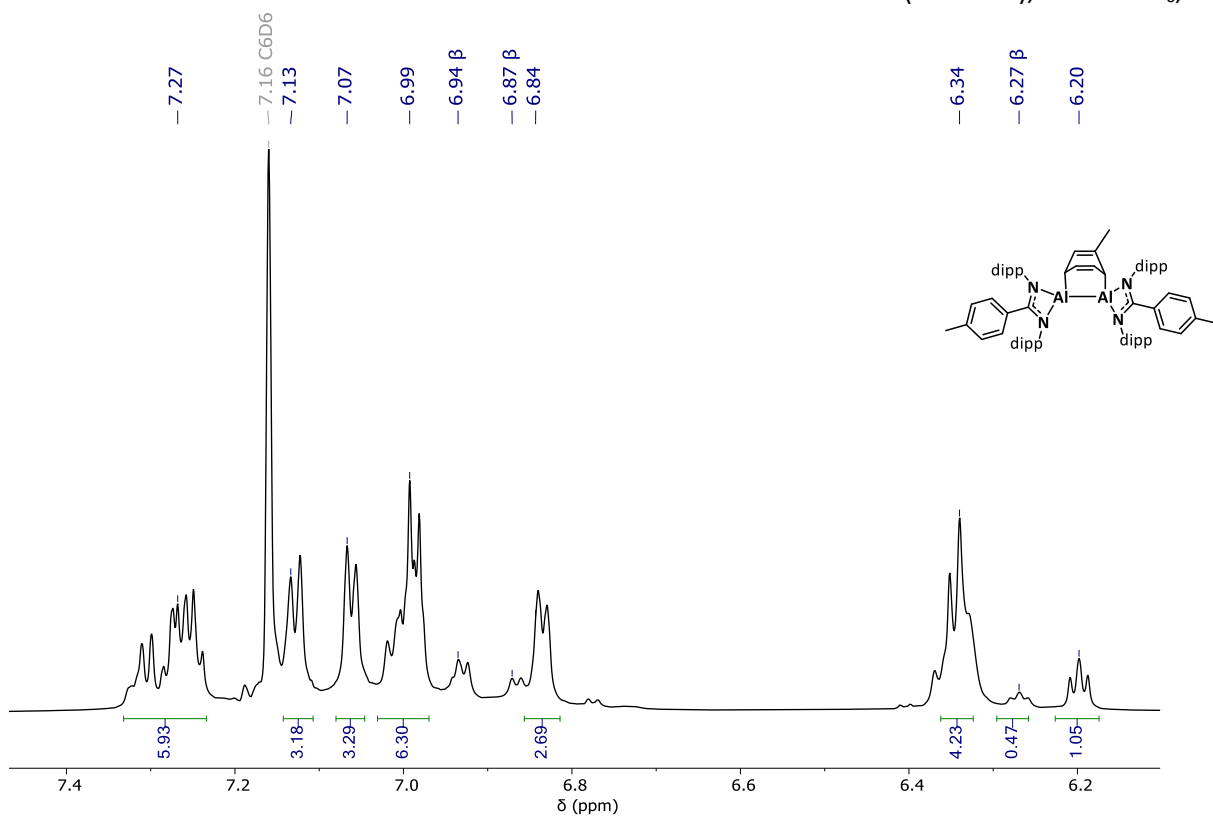
Figure S39: 'Aryl region' (6-7.4 ppm) of ^{1}H NMR spectrum of compound **2**
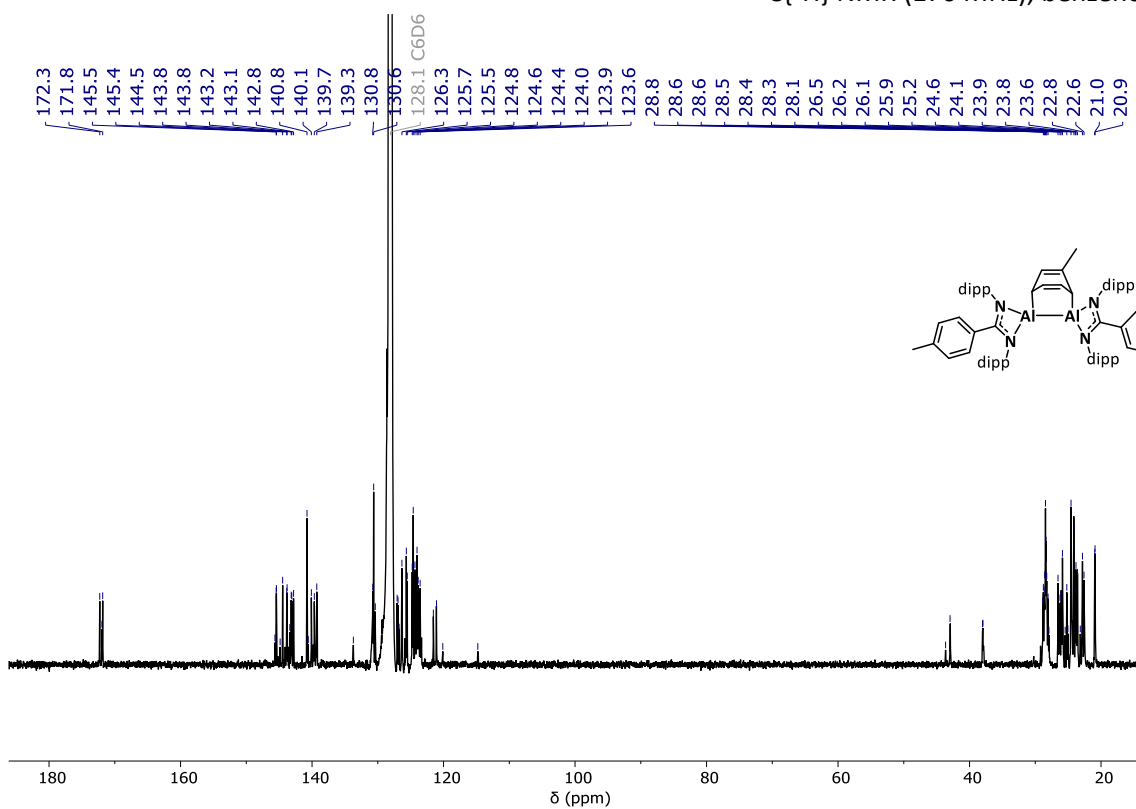
Figure S40: ^{13}C{^{1}H} NMR spectrum of compound **2**
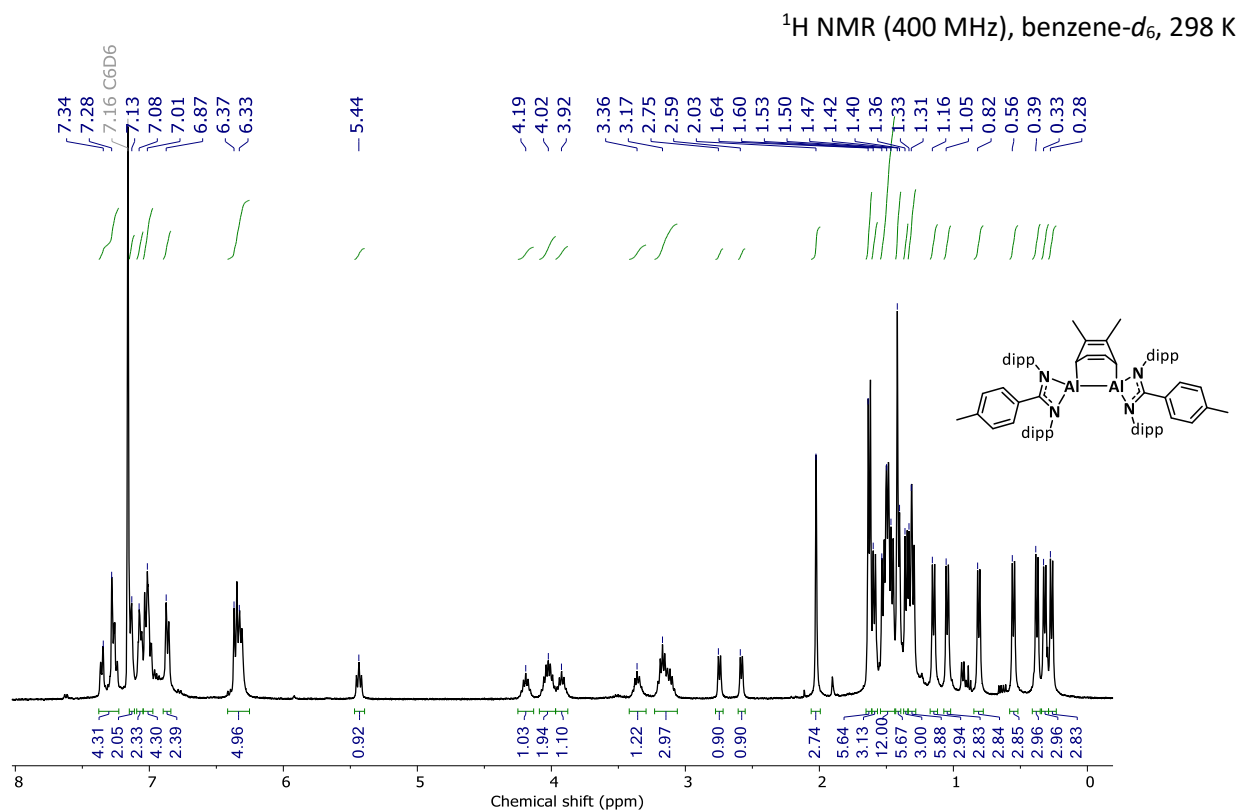
Figure S41: ^{1}H NMR spectrum of compound **3**
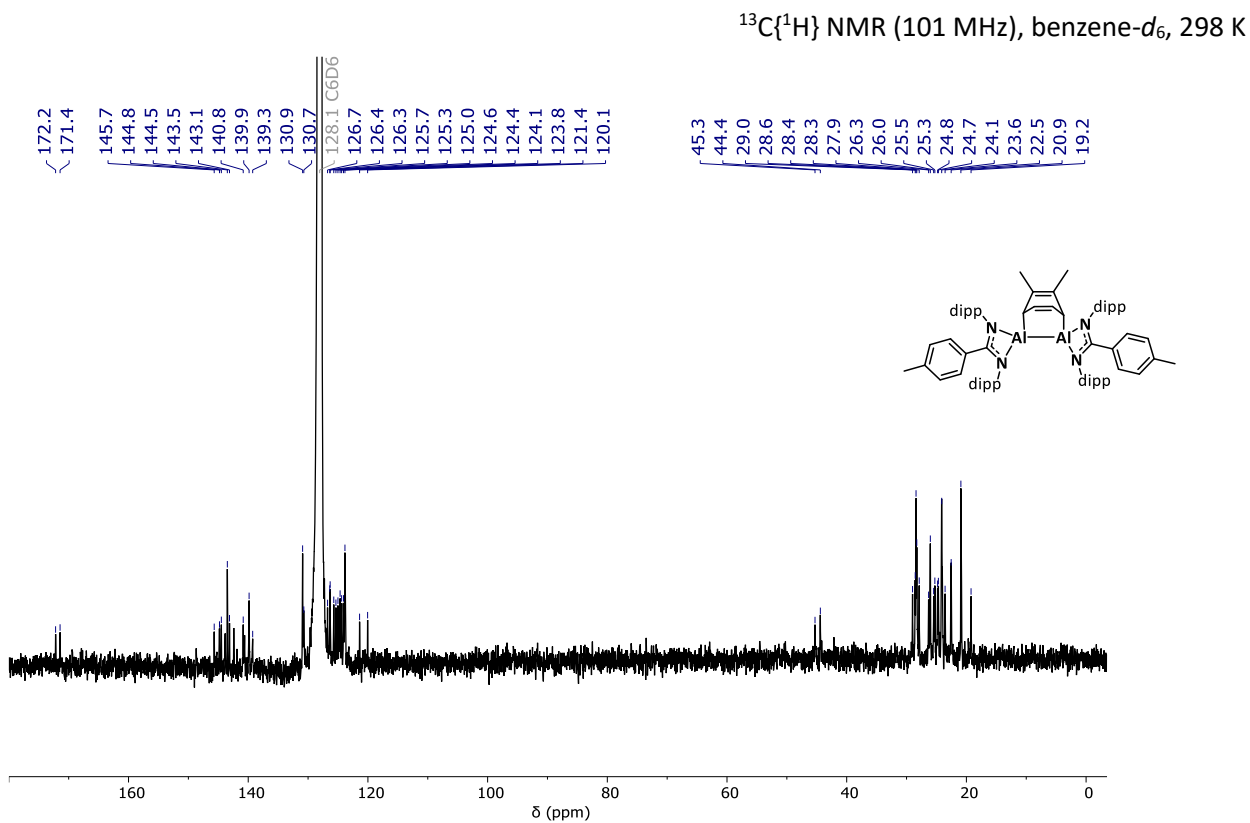
Figure S42: ^{13}C{^{1}H} NMR spectrum of compound **3**
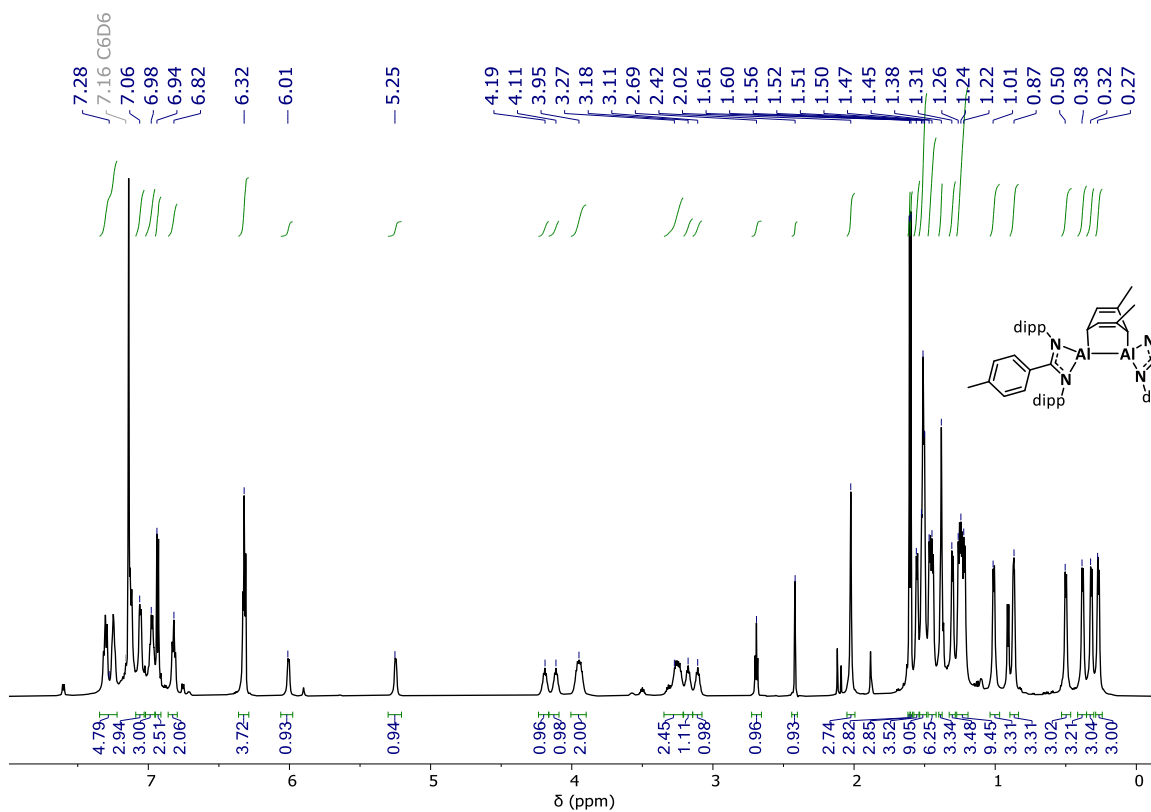
Figure S43: ^{1}H NMR spectrum of compound **4**

Figure S44: ^{13}C{^{1}H} NMR spectrum of compound **4**
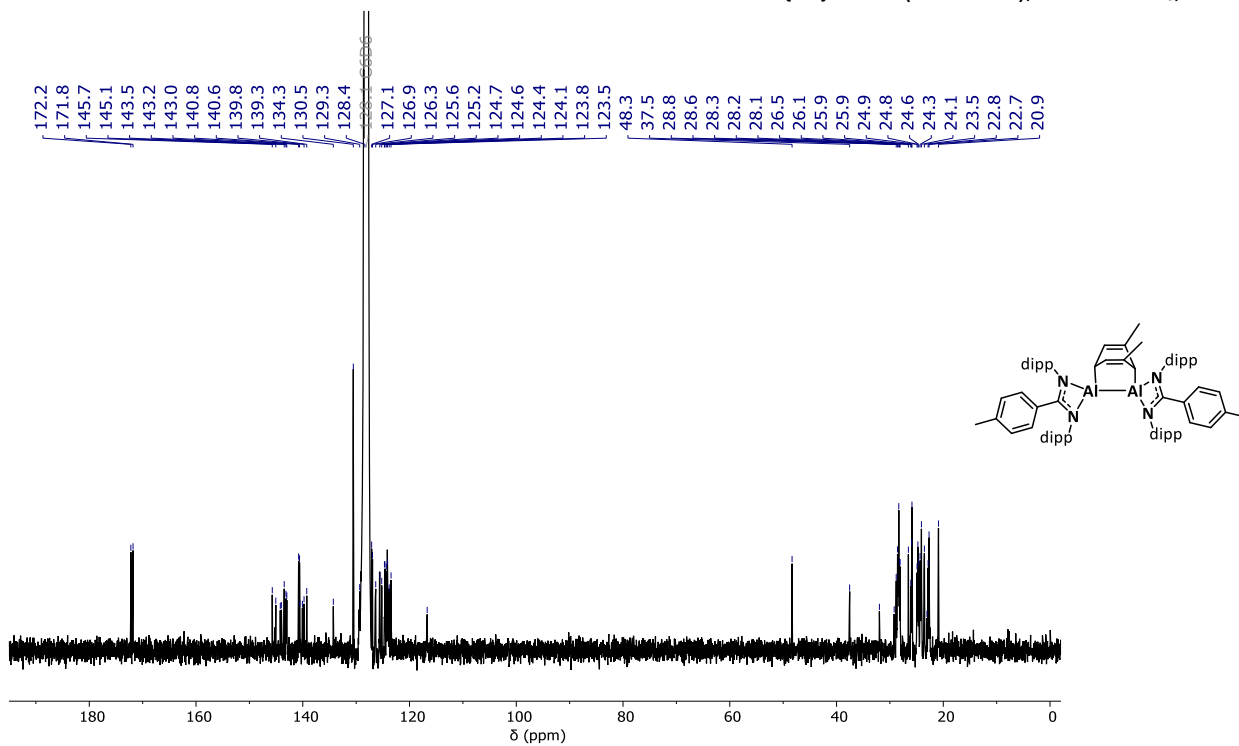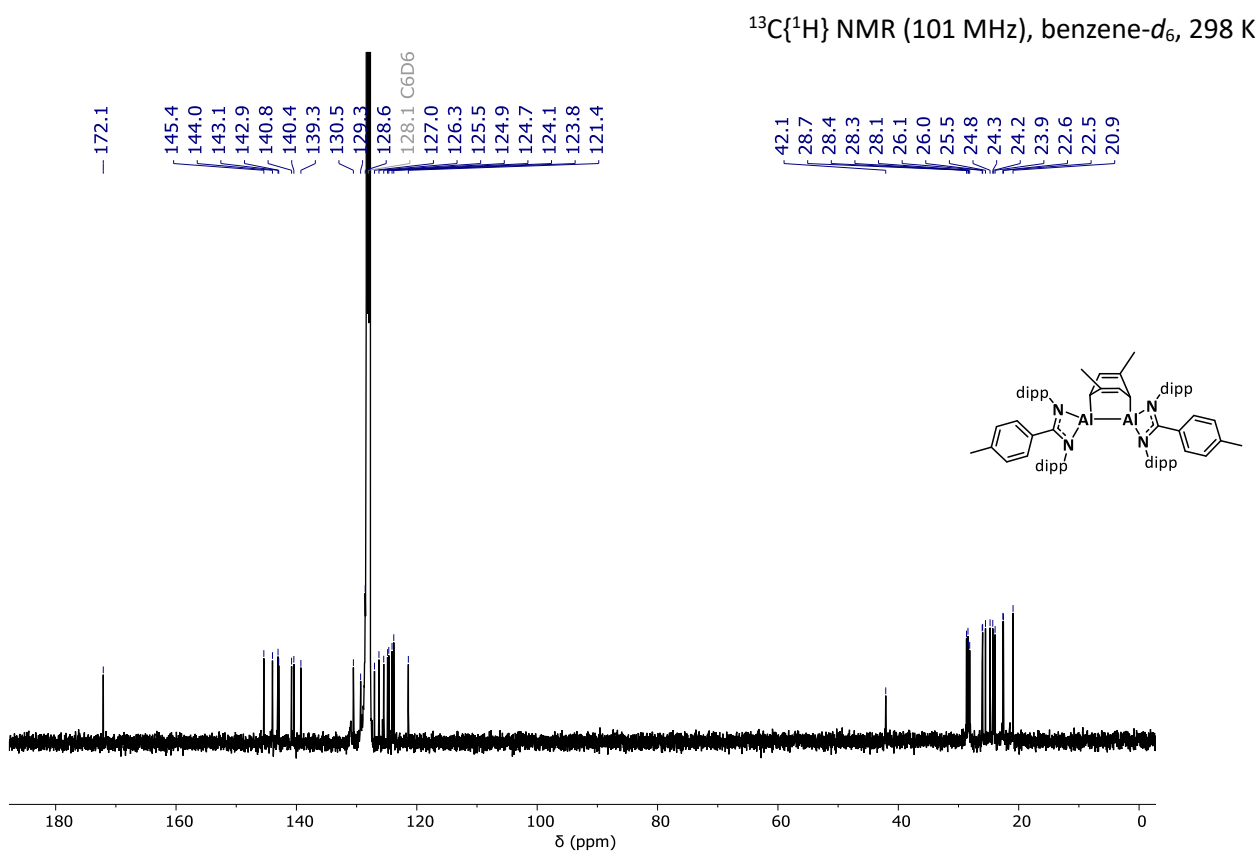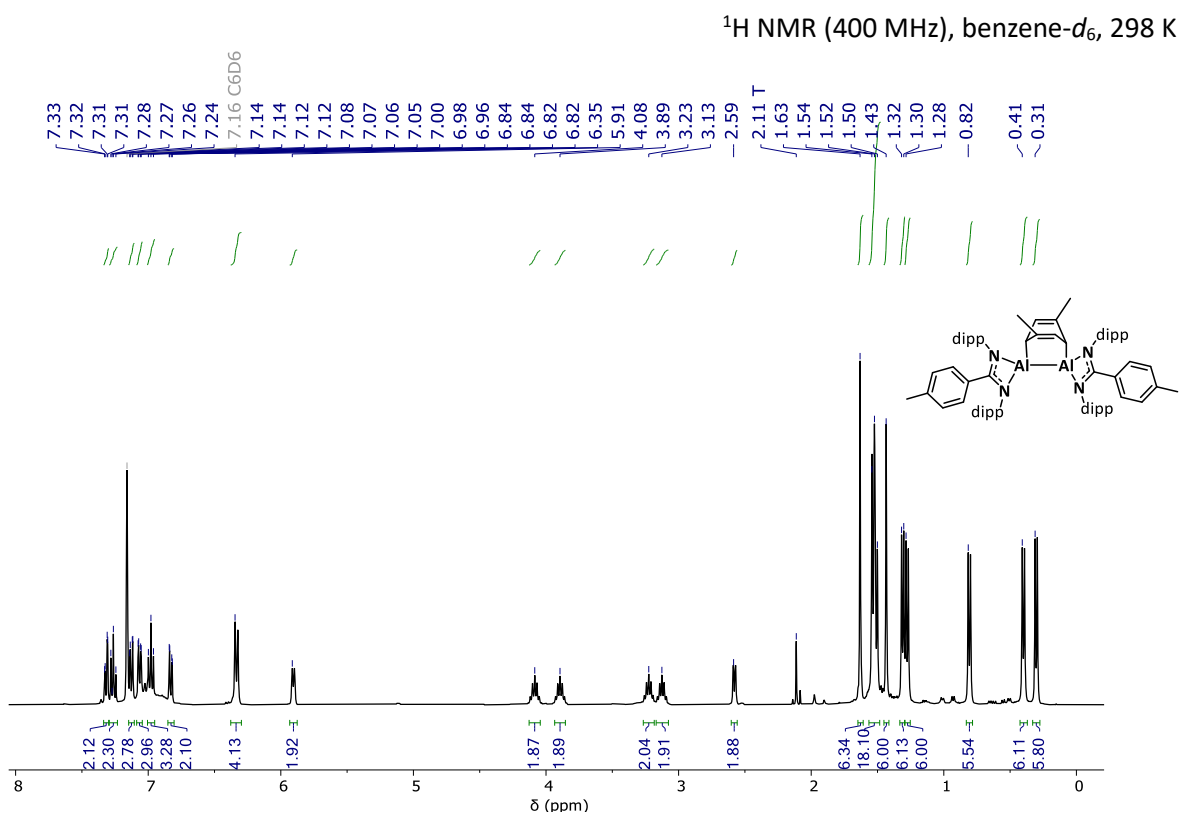
Figure S45: ^{1}H NMR spectrum of compound **5**

Figure S46: ^{13}C{^{1}H} NMR spectrum of compound **5**

7. References

1   J. K. Ruff and M. F. Hawthorne, *J. Am. Chem. Soc.*, 1960, **82**, 2141–2144.
2   C. Cui, H. W. Roesky, H.-G. Schmidt, M. Noltemeyer, H. Hao and F. Cimpoesu, *Angew. Chem. Int. Ed.*, 2000, **39**, 4274–4276.
3   K. Hobson, C. J. Carmalt and C. Bakewell, *Inorg. Chem.*, 2021, **60**, 10958–10969.
4   C. Bakewell, K. Hobson and C. J. Carmalt, *Angew. Chem. Int. Ed.*, 2022, **61**, e202205901.
5   T. Chu, I. Korobkov and G. I. Nikonov, *J. Am. Chem. Soc.*, 2014, **136**, 9195–9202.
6   S. J. Bonyhady, D. Collis, G. Frenking, N. Holzmann, C. Jones and A. Stasch, *Nat. Chem.*, 2010, **2**, 865–869.
7   R. K. Brown, T. N. Hooper, F. Rekhroukh, A. J. P. White, P. J. Costa and M. R. Crimmin, *Chem. Commun.*, 2021, **57**, 11673–11676.
8   O. V. Dolomanov, L. J. Bourhis, R. J. Gildea, J. A. K. Howard and H. Puschmann, *J. Appl. Cryst.*, 2009, **42**, 339–341.
9   G. M. Sheldrick, *Acta Crystallogr. A*, 2015, **71**, 3–8.
10   G. M. Sheldrick, *Acta Crystallogr. C*, 2015, **71**, 3–8.
11   W. J. Hehre, R. Ditchfield and J. A. Pople, *J. Chem. Phys.*, 1972, **56**, 2257–2261.
12   P. C. Hariharan and J. A. Pople, *Theoret. Chim. Acta*, 1973, **28**, 213–222.
13   T. Clark, J. Chandrasekhar, G. W. Spitznagel and P. V. R. Schleyer, *J. Comput. Chem.*, 1983, **4**, 294–301.
14   J. Tomasi, B. Mennucci and R. Cammi, *Chem. Rev.*, 2005, **105**, 2999–3094.
15   J.-D. Chai and M. Head-Gordon, *J. Chem. Phys.*, 2008, **128**, 084106.
16   E. D. Glendening, C. R. Landis and F. Weinhold, *J. Comput. Chem.*, 2013, **34**, 1429–1437.
17   F. Weinhold and C. R. Landis, *Chem. Educ. Res. Pract.*, 2001, **2**, 91–104.
18   T. A. Keith, AIMALL (version 19.10.12) TK Gristmill Software, Overland Park, KS, USA, 2019.